UNIVERSITÀ DEGLI STUDI DI VERONA

Physical Human Robot Interaction Report

COMPUTER ENGINEERING FOR ROBOTICS AND SMART INDUSTRY

Nicola Marchiotto - VR462317

2022

Contents

1 Four Channel Bilateral Teleoperation

1.1 Continuous Four Channel Bilateral Teleoperation

Description: Implement the Single-Input Single-Output Four-channel bilateral teleoperation architecture with

$$C_m = B_m + \frac{K_m}{s} \quad C_s = B_s + \frac{K_s}{s}$$
$$Z_m{}^{-1} = \frac{1}{M_m s} \quad Z_s^{-1} = \frac{1}{M_s s}$$

where $M_m = 0.5$ and $M_s = 2$

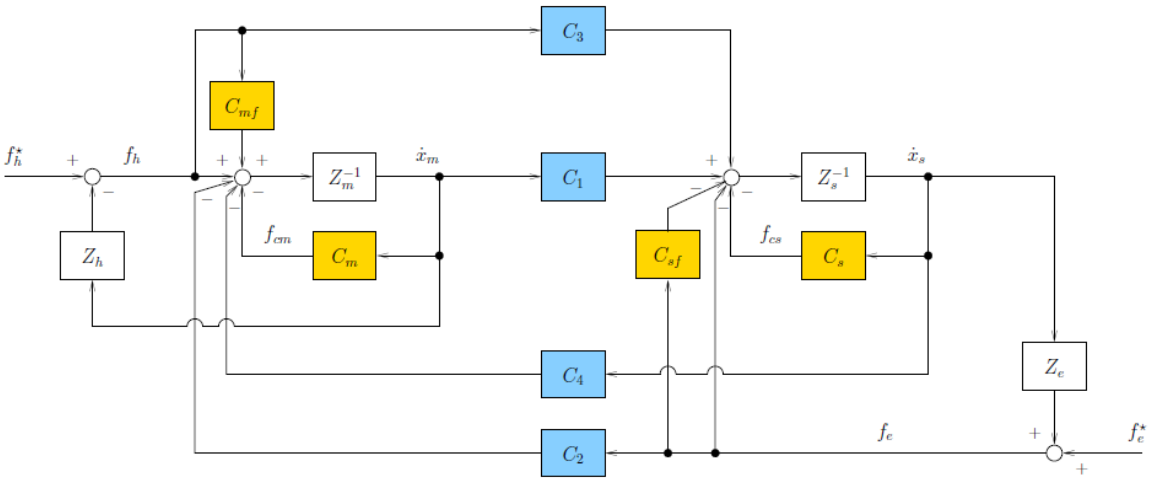

Figure 1: Four channel bilateral teleoperation architecture with local force feedbacks

To obtain perfect transparency, the coordination controllers were set to

$$C_1 = Z_s + C_s \quad C_2 = C_3 = I \quad C_4 = -(Z_m + C_m)$$

The implemented architecture was tested with sinuisoidal reference signal with frequency π

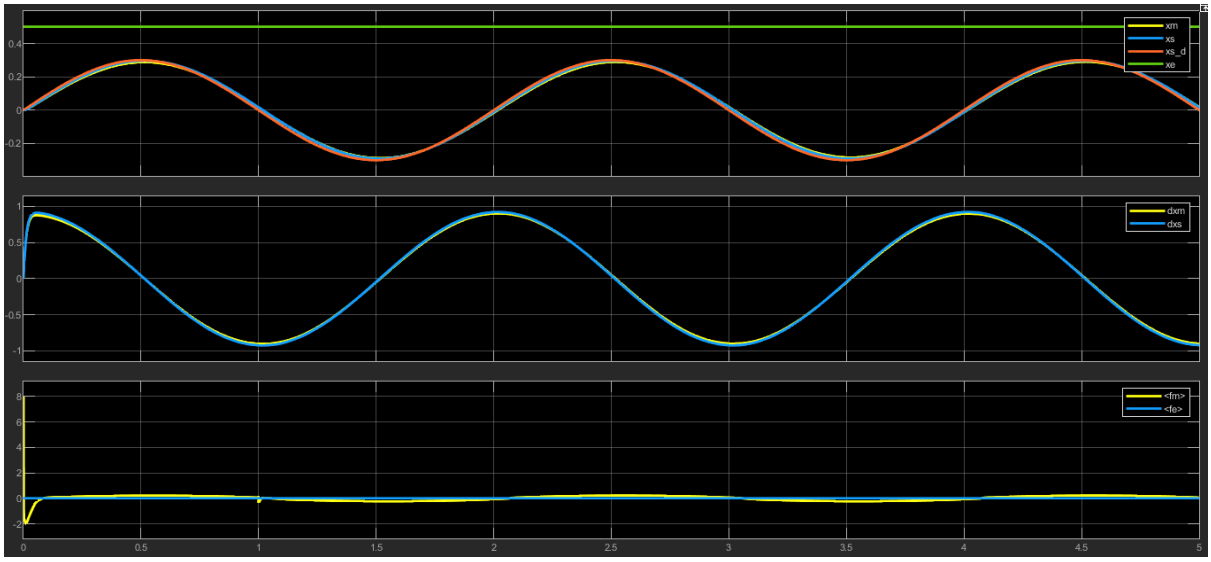

Figure 2: 4 channel bilateral architecture with a sinusoidal reference in free motion

Full transparency was obtained as shown by the force plot in the following figure upon contact. The environment was modelled as a pure stiffness with $K_e = 200$ and located at $x_e = 0.5$

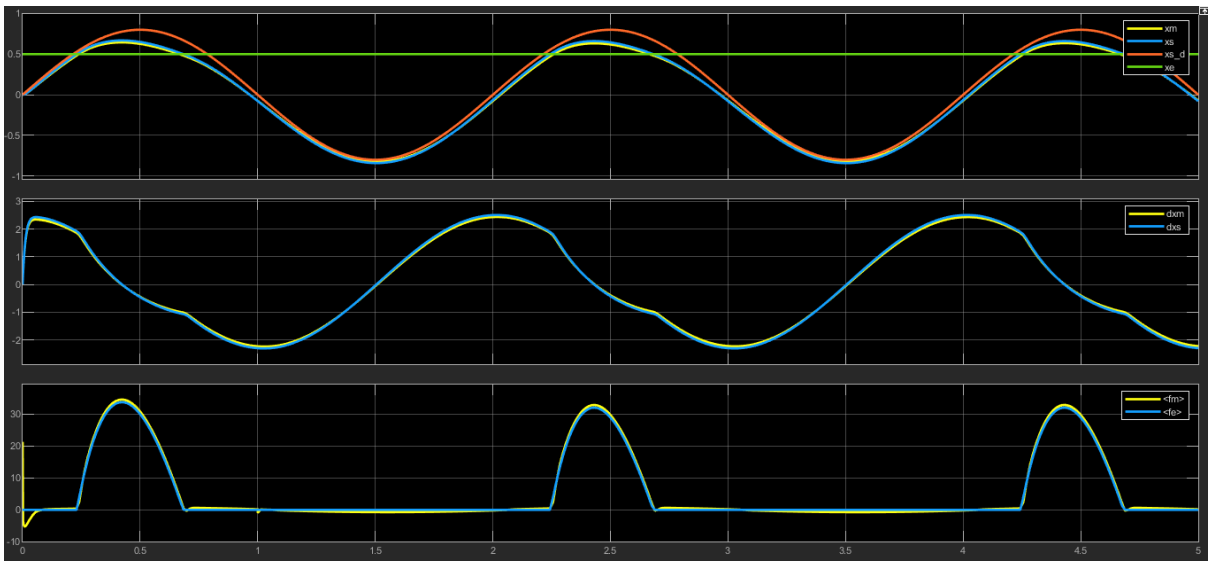

Figure 3: 4 channel bilateral architecture with a sinusoidal reference in contact

To test the performance of the architecture, a step reference signal was provided.

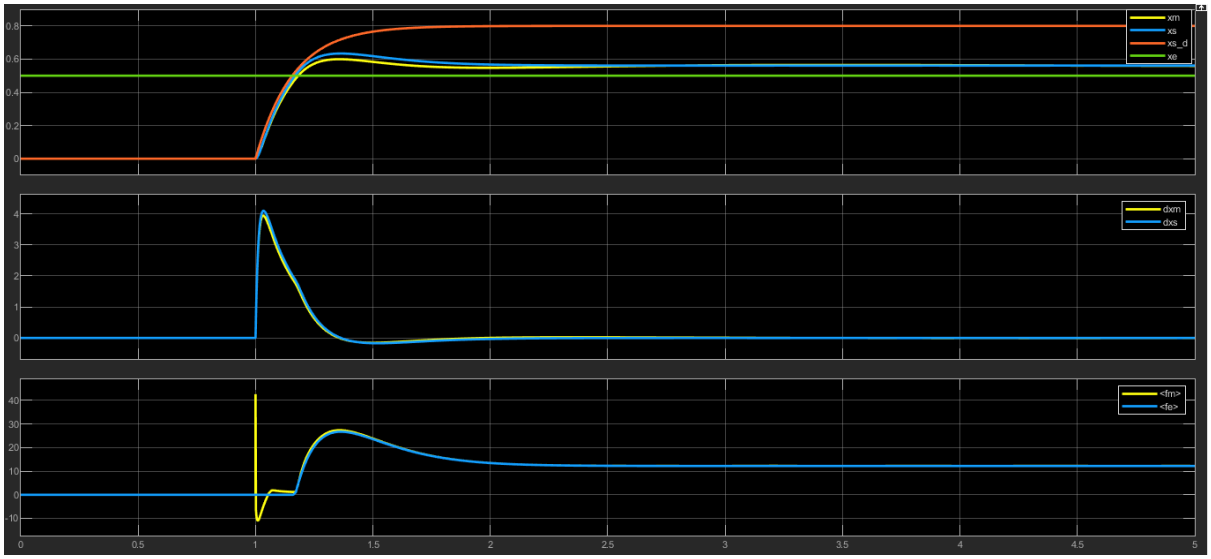

Figure 4: 4 channel bilateral architecture with a step reference in contact

1.2 Discrete Four Channel Bilateral Teleoperation with Kalman Estimation and local force feedbacks

Description: Discretize the Single-Input Single-Output Four-channel bilateral teleoperation architecture, add measurement noise to the position/force signals and estimated the velocities from positions. Then add local force feedback

Force and position feedbacks act in opposite ways, in the sense that one softens and the other stiffens the sender device

When the slave is in contact with a hard environment, contact force is the dominant signal for transmission and local force/position control has to be amplified/attenuated

When the slave is in free motion or in contact with a soft environment, position or velocity is the dominant signal for transmission and local position/force control has to be amplified/attenuated

The coordination controllers were set to

$$C_1 = Z_s + C_s \quad C_2 = 1 + C_{mf} \quad C_3 = 1 + C_{sf} \quad C_4 = -(Z_m + C_m)$$

The following figures show how the architecture with local force feedbacks react to a step reference signal, the noise addition was omitted to better show the differences in the two cases

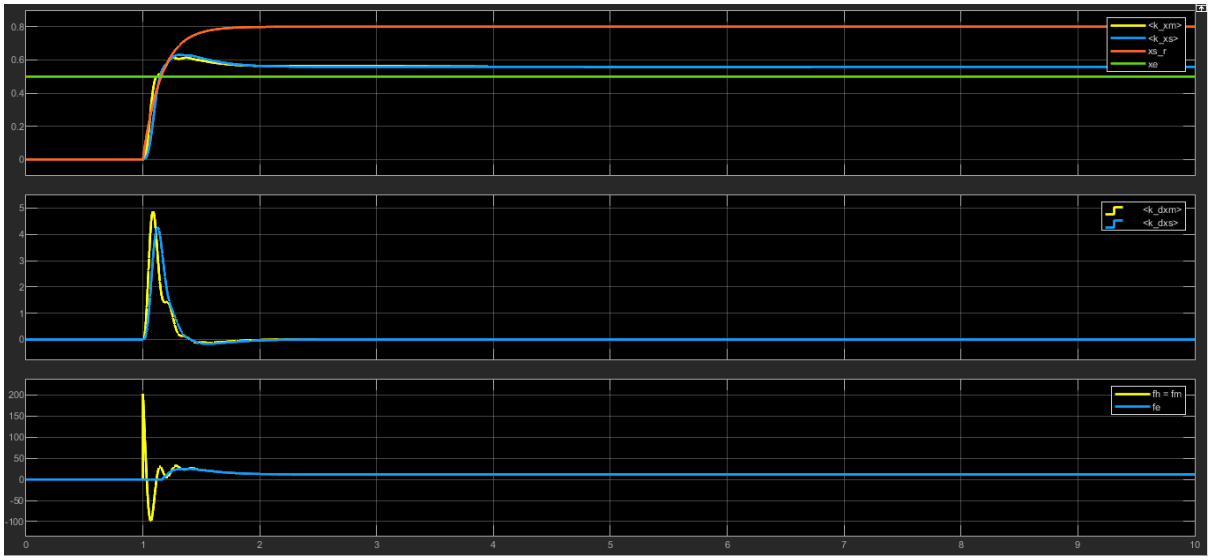

Figure 5: 4 channel bilateral architecture with local force feedbacks, $C_{mf} = 0, C_{sf} = 0$

As can be seen from the following figure, using a local force feedback as a proportional gain $C_{sf} = 10$, the slave side perceive a harder encironment w.r.t. the master side

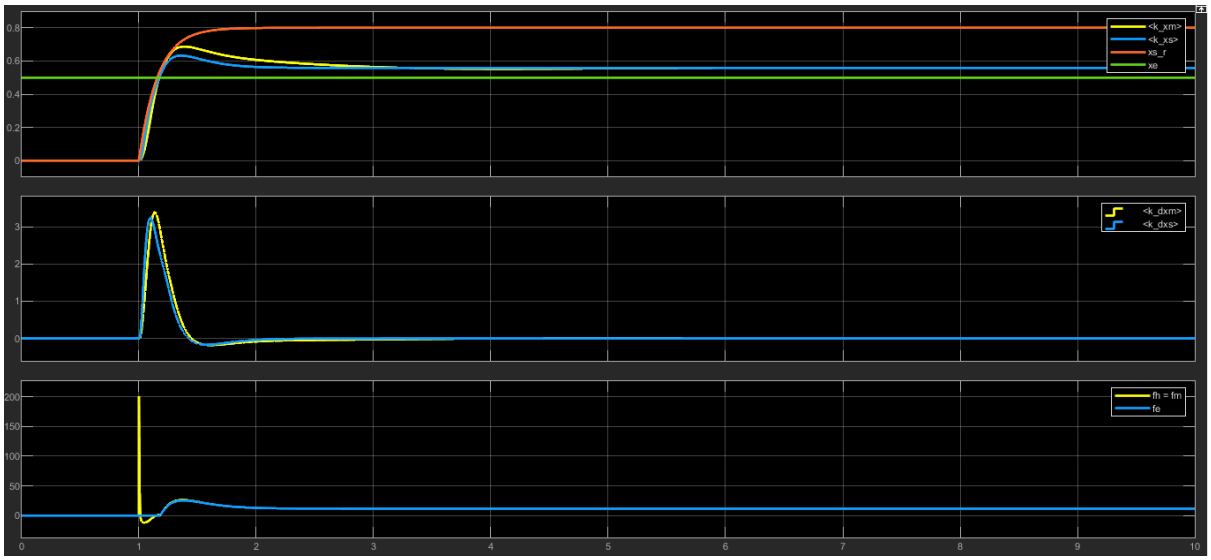

Figure 6: 4 channel bilateral architecture with local force feedbacks, $C_{mf} = 0, C_{sf} = 10$

To estimate position from velocities, the kalman filter was used both at master and slave side. Position and Force noise were simulated, the following figures show noisy and estimated position and velocity at the master side when a reference step signal is provided. The showed behaviour is in free motion

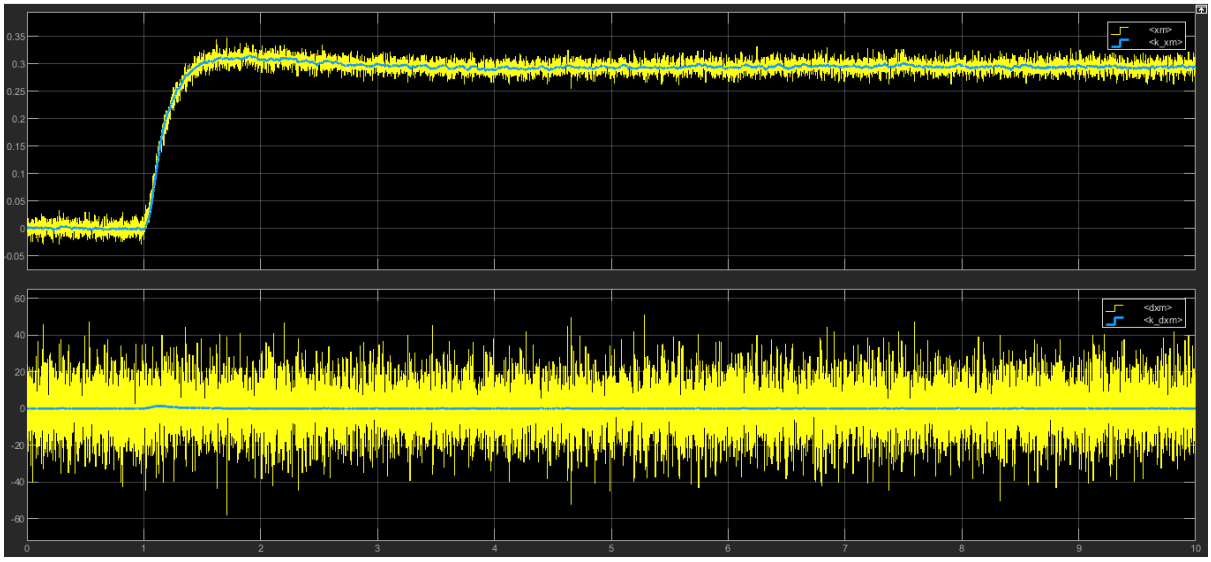

Figure 7: Comparison between noisy signals and estimated signals using kalman filter

The implemented architecture was tested with sinuisoidal reference signal with frequency π

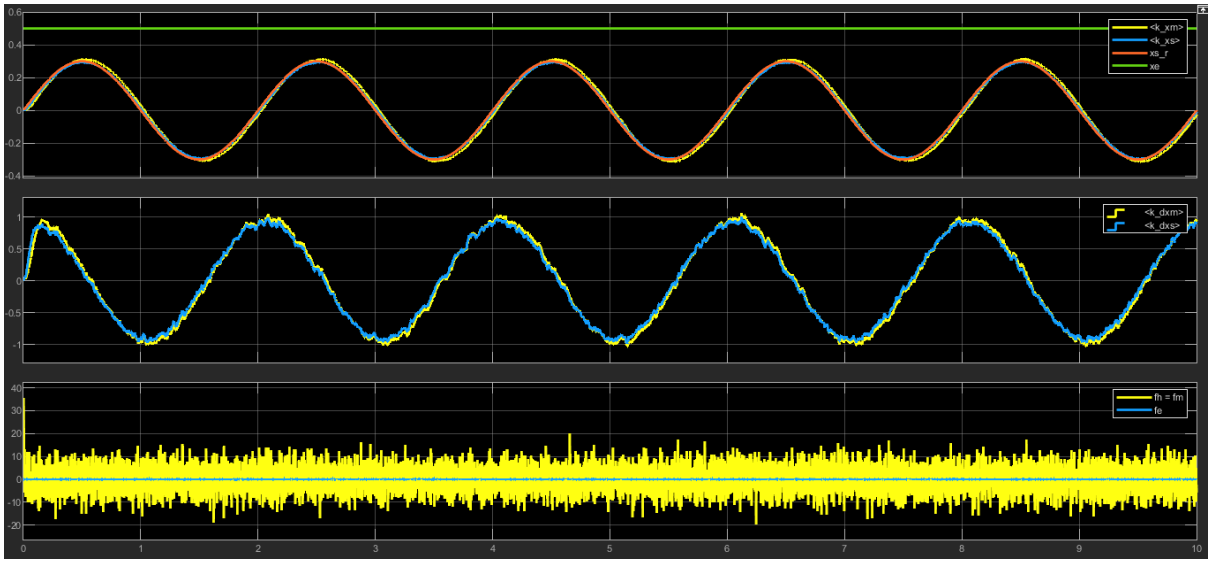

Figure 8: Discretized 4 channel bilateral architecture with a sinusoidal reference in free motion

Full transparacy was obtained as shown by the force plot in the following figure upon contact. The environment was modelled as a pure stiffness with $K_e = 200$ and located at $x_e = 0.5$

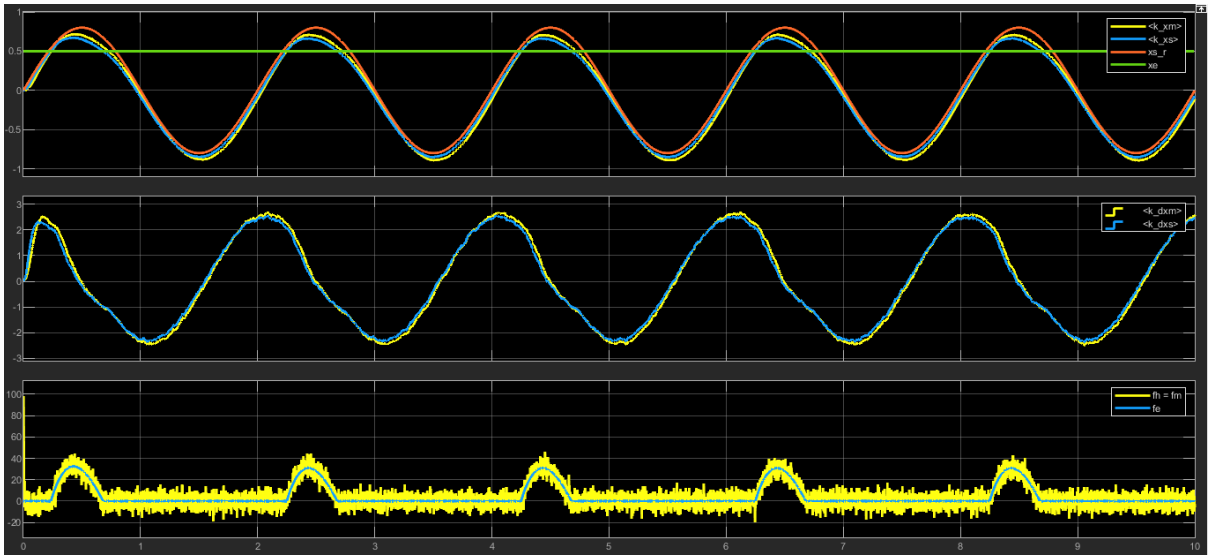

Figure 9: Discretized 4 channel bilateral architecture with a sinusoidal reference in contact

To test the performance of the architecture, a step reference signal was provided.

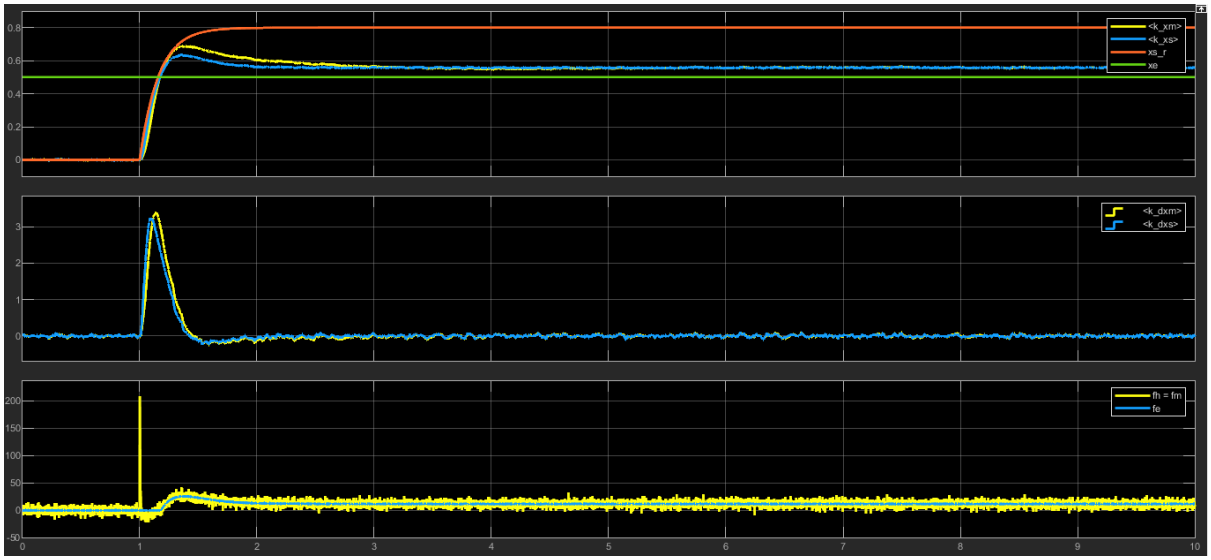

Figure 10: Discretized 4 channel bilateral architecture with a step reference in contact

1.3 Derivation of the hybrid matrix considering local force feedbacks

Description: Derive the expression for the hybrid matrix H of the Four Channel Bilateral Teleoperation architecture with local force feedbacks

Hybrid transfer matrix

From the expression

$$\begin{bmatrix} f_m \\ \dot{x}_m \end{bmatrix} = \begin{bmatrix} H_{11}(s) & H_{12}(s) \\ H_{21}(s) & H_{22}(s) \end{bmatrix} \begin{bmatrix} \dot{x}_s \\ -f_s \end{bmatrix}$$

it is easy to compute each elements of the hybrid matrix (Lawrence) as a function of the controllers $(C_m, C_s, C_1, \ldots, C_4)$ and the master/slave robot impedance (Z_m, Z_s)

$$\begin{aligned} H_{11} &:= \left.\frac{f_m}{\dot{x}_s}\right|_{f_s=0} = (Z_m + C_m)D(Z_s + C_s - C_3C_4) + C_4 \\ H_{12} &:= -\left.\frac{f_m}{f_s}\right|_{\dot{x}_s=0} = -(Z_m + C_m)D(I - C_3C_2) - C_2 \\ H_{21} &:= \left.\frac{\dot{x}_m}{\dot{x}_s}\right|_{f_s=0} = D(Z_s + C_s - C_3C_4) \\ H_{22} &:= -\left.\frac{\dot{x}_m}{f_s}\right|_{\dot{x}_s=0} = -D(I - C_3C_2) \end{aligned}$$

where $D = (C_1 + C_3Z_m + C_3C_m)^{-1}$.

4-Channel Bilateral Teleoperation Riccardo Muradore 13

Four-Channel with local force loops

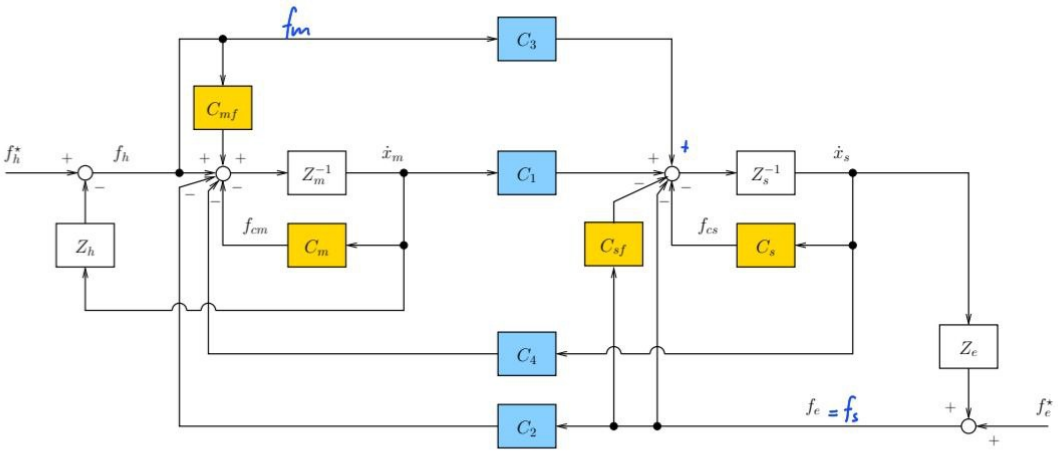

Hashtrudi-Zaad, Salcudean 2001

4-Channel Bilateral Teleoperation Riccardo Muradore 37

$$\begin{bmatrix} f_m \\ \dot{x}_m \end{bmatrix} = \begin{bmatrix} H_{11}(s) & H_{12}(s) \\ H_{21}(s) & H_{22}(s) \end{bmatrix} \begin{bmatrix} \dot{x}_s \\ -f_s \end{bmatrix}$$

$Z_{cm} \triangleq Z_m + C_m$

$Z_{cs} \triangleq Z_s + C_s$

① $f_m = H_{11}(s)\,\dot{x}_s$ with $f_s = 0$, $H_{11}(s) = \dfrac{f_m}{\dot{x}_s}$

$$\frac{f_m(1 + C_m f) - C_4 \dot{x}_s - \dot{x}_m C_m - C_2 f_s}{Z_m} = \dot{x}_m$$

$$f_m(1 + C_m f) - C_4 \dot{x}_s - \dot{x}_m C_m - C_2 f_s = \dot{x}_m Z$$

$$\frac{f_m(1 + C_m f) - C_4 \dot{x}_s - C_2 f_s}{C_m + Z_m} = \dot{x}_m$$

Computation for retrieving $\dot{x}_m$ to simplify the above equation

$$\dot{X}_s = \frac{C_3 f_m + C_1 \dot{x}_m - f_e(1 + C_s f) - C_s \dot{x}_s}{Z_s}$$

$$\dot{x}_s Z_s + \dot{x}_s C_s = C_3 f_m + C_1 \dot{x}_m - f_e(1 + C_s f)$$

$$\dot{x}_s(Z_s + C_s) = C_3 f_m + C_1 \dot{x}_m - f_e(1 + C_s f)$$

$$\dot{x}_m = \frac{\dot{x}_s(Z_s + C_s) - C_3 f_m + f_e(1 + C_s f)}{C_1},$$

$$\dot{x}_s = \frac{C_3 f_m + C_1 \dot{x}_m - f_e(1 + C_s f)}{Z_{cs}}$$

$\longrightarrow$ Substituting in eq * we get $\longrightarrow H_{11}(s) = \frac{f_m}{\dot{x}_s}$

$$\frac{f_m(1+C_m f)\cdot C_4\dot{x}_s - C_2 f_s}{C_m + Z_m} = \frac{\dot{x}_s(Z_s + C_s) - C_3 f_m - f_e(1+C_s f)}{C_1}$$

$$C_1 f_m(1 + C_m f) - C_1(C_4\dot{x}_s - C_2 f_s) = \dot{x}_s(C_m+Z_m)(Z_s + C_s) - (C_m+Z_m)\left[(C_3 f_m) - f_e(1+C_s f)\right]$$

$$C_1 f_m(1 + C_m f) - C_1(C_4\dot{x}_s - C_2 f_s) = \dot{x}_s Z_{cm} Z_{cs} - Z_{cm} C_3 f_m + Z_{cm} f_e(1 + C_s f)$$

$$f_m\left[C_1(1+C_m f) + Z_{cm} C_3\right] = \dot{x}_s\left(Z_{cm} Z_{cs} + C_1 C_4\right) - f_s\left(C_1 C_2 + Z_{cm}(1+C_s f)\right)$$

$$\frac{f_m}{\dot{x}_s} = \frac{Z_{cm} Z_{cs} + C_1 C_4 - f_s\left(C_1 C_2 + Z_{cm}(1+C_s f)\right)}{C_1(1+C_m f) + C_3 Z_{cm}}$$

$$\left.\frac{f_m}{\dot{x}_s}\right|_{f_s=0} = \frac{Z_{cm} Z_{cs} + C_1 C_4}{C_1(1+C_m f) + C_3 Z_{cm}} = H_{11} \quad \checkmark$$

$\longrightarrow$ Confronting with H_{11} of the hybrid matrix $\hat{H}$ without local feedback

$$\hat{H}_{11} = \frac{(Z_m + C_m)(Z_s + C_s - C_3 C_4)}{C_1 + C_3(Z_m + C_m)} + C_4 =$$

$$= \frac{Z_{cm} Z_{cs} - \cancel{Z_{cm} C_3 C_4} + C_1 C_4 \pm \cancel{C_3 C_4 Z_{cm}}}{C_1 + C_3 Z_{cm}}$$

$$= \frac{Z_{cm} Z_{cs} + C_1 C_4}{C_1 + C_3 Z_{cm}}$$

② $H_{12} = -\frac{f_m}{f_s}$ $\quad \dot{x}_s = 0$

$$C_1 f_m (1 + C_{mf}) - C_1 (C_1 \dot{x}_s - C_2 f_s) = \dot{x}_s (C_m Z_m)(Z_s + C_s) - (C_m Z_m)\left[(C_3 f_m) - f_e (1 + C_{sf})\right]$$

$$C_1 f_m (1 + C_{mf}) - C_1 C_2 f_s = -Z_{cm} C_3 f_m + Z_{cm} f_s (1 + C_{sf})$$

$$f_m \left[C_1 (1 + C_{mf}) + Z_{cm} C_3 \right] = f_s \left[C_1 C_2 + Z_{cm} (1 + C_{sf}) \right]$$

$$-\left.\frac{f_m}{f_s}\right|_{\dot{x}_s = 0} = -\frac{C_1 C_2 + Z_{cm} (1 + C_{sf})}{C_1 (1 + C_{mf}) + Z_{cm} C_3} = H_{12} \quad \checkmark$$

→ Confronting with H_{12} of the hybrid matrix $\hat{H}$ without local feedback

$$H_{12} = -\frac{Z_{cm} (1 - C_3 C_2)}{C_1 + C_3 Z_{cm}} \quad - C_2 = \frac{-Z_{cm} (1 - C_3 C_2) - C_2 (C_1 + C_3 Z_{cm})}{C_1 + C_3 Z_{cm}}$$

$$= \frac{-Z_{cm} + Z_{cm} C_3 C_2 - C_1 C_2 - C_2 C_3 Z_{cm}}{C_1 + C_3 Z_{cm}}$$

$$= -\frac{C_1 C_2 + Z_{cm}}{C_1 + C_3 Z_{cm}}$$

(3) $H_{21} = \left.\frac{\dot{x}_m}{\dot{x}_s}\right|_{f_s=0}$

$\dot{x}_m = \frac{\dot{x}_s (Z_s + C_s) - C_3 f_m + f_s (1 + C_s f)}{C_1}$

$\dot{x}_m = \frac{\dot{x}_s Z_{cs}}{C_1} - \frac{C_3}{C_1} f_m$

Using : $\frac{f_m}{\dot{x}_s} = \frac{Z_{cm} Z_{cs} + C_1 C_4 - f_s (C_1 C_2 + Z_{cm} (1 + C_s f))}{C_1 (1 + C_{mf}) + C_3 Z_{cm}}$

$\left.\frac{\dot{x}_m}{\dot{x}_s}\right|_{f_s=0} = \frac{Z_{cs}}{C_1} - \frac{C_3}{C_1} \left(\frac{Z_{cm} Z_{cs} + C_1 C_4}{C_1 (1 + C_{mf}) + C_3 Z_{cm}} \right)$

$= \frac{Z_{cs} C_1 (1 + C_{mf}) + Z_{cs} C_3 Z_{cm} - C_3 Z_{cm} Z_{cs} - C_1 C_4 C_4}{C_1 \left(C_1 (1 + C_{mf}) + C_3 Z_{cm} \right)}$

$= \frac{Z_{cs} (1 + C_{mf}) - C_3 C_4}{C_1 (1 + C_{mf}) + C_3 Z_{cm}} = H_{21}$ ✓

→ Confronting with H_{21} of the hybrid matrix $\hat{H}$ without local feedback

$H_{21} = \frac{Z_{cs} - C_3 C_4}{C_1 + C_3 Z_{cm}}$

(4) $H_{22} = \left. -\frac{\dot{x}_m}{f_s} \right|_{\dot{x}_s = 0}$ $\qquad \hat{H}_{22} = \frac{1 - C_3 C_2}{C_1 + C_3 Z_{cm}}$

$$\dot{x}_m = \frac{\dot{x}_m (Z_s + C_s) - C_3 f_m + f_s (1 + C_s f)}{C_1}$$

Using $\left. \frac{f_m}{f_s} \right|_{\dot{x}_s = 0} = \frac{C_1 C_2 + Z_{cm}(1 + C_s f)}{C_1 (1 + C_m f) + Z_{cm} C_3}$ we get

$$\left. \frac{\dot{x}_m}{f_s} \right|_{\dot{x}_s = 0} = -\frac{C_3}{C_1} \left(\frac{C_1 C_2 + Z_{cm}(1 + C_s f)}{C_1 (1 + C_m f) + Z_{cm} C_3} \right) + \frac{1 + C_s f}{C_1}$$

$$= \frac{-C_1 C_2 C_3 - Z_{cm} C_3 - Z_{cm} C_3 C_s f + C_1 (1 + C_m f)(1 + C_s f) + Z_{cm} C_3 (1 + C_s f)}{C_1 (C_1 (1 + C_m f) + Z_{cm} C_3)}$$

$$= \frac{-\cancel{C_1 C_2 C_3} - \cancel{Z_{cm} C_3} - \cancel{Z_{cm} C_3 C_s f} + \cancel{C_1} + \cancel{C_1 C_s f} + \cancel{C_1 C_m f} + \cancel{C_1 C_m f C_s f} + \cancel{Z_{cm} C_3} + \cancel{Z_{cm} C_3 C_s f}}{\cancel{C_1} (C_1 (1 + C_m f) + Z_{cm} C_3)}$$

$$= \frac{1 - C_2 C_3 + C_s f + C_m f + C_m f C_s f}{C_1 (1 + C_m f) + Z_{cm} C_3} = H_{22} \quad \checkmark$$

→ Confronting with H_{22} of the hybrid matrix $\hat{H}$ without local feedback

$$\hat{H}_{22} = \frac{1 - C_3 C_2}{C_1 + C_3 Z_{cm}}$$

- Final Recap

$$Z_{cm} \triangleq Z_m + C_m$$
$$Z_{cs} \triangleq Z_s + C_s$$

$$H_{11} = \frac{Z_{cm} Z_{cs} + C_1 C_4}{C_1 (1 + C_{mf}) + C_3 Z_{cm}}$$

$$H_{12} = -\frac{C_1 C_2 + Z_{cm} (1 + C_{sf})}{C_1 (1 + C_{mf}) + Z_{cm} C_3}$$

$$H_{21} = \frac{Z_{cs} (1 + C_{mf}) - C_3 C_4}{C_1 (1 + C_{mf}) + C_3 Z_{cm}}$$

$$H_{22} = \frac{1 - C_2 C_3 + C_{sf} + C_{mf} + C_{mf} C_{sf}}{C_1 (1 + C_{mf}) + Z_{cm} C_3}$$

2 Statistical filtering

Given the measurement equation $y(t) = s(t) + n(t)$ where

- $y(t)$ is the measurement at time t
- $s(t)$ is the signal we are interested in
- $n(t)$ is the additive measurement noise

We will tackle the following estimation problems:

- **Filtering:** optimal estimate $\hat{s}(t)$ of $s(t)$ using measurements $y(\cdot)$ till time t
- **Prediction:** optimal estimate $\hat{s}(t+h)$ of $s(t+h)$ measurements y till instant t
- **Smoothing:** optimal estimate $\hat{s}(t-h)$ of $s(t-h)$ measurements y till instant t

2.1 Kalman filter, predictor and smoother

Description: Implement the Kalman filter/predictor, Kalman smoother and estimate the velocity and acceleration from noisy position measurements

The following figures compare position, velocity and acceleration estimated using the kalman filter, predictor and smoother with the measured position and velocity and with the acceleration computed via euler approximation and processed with a low pass filter at 5 Hz

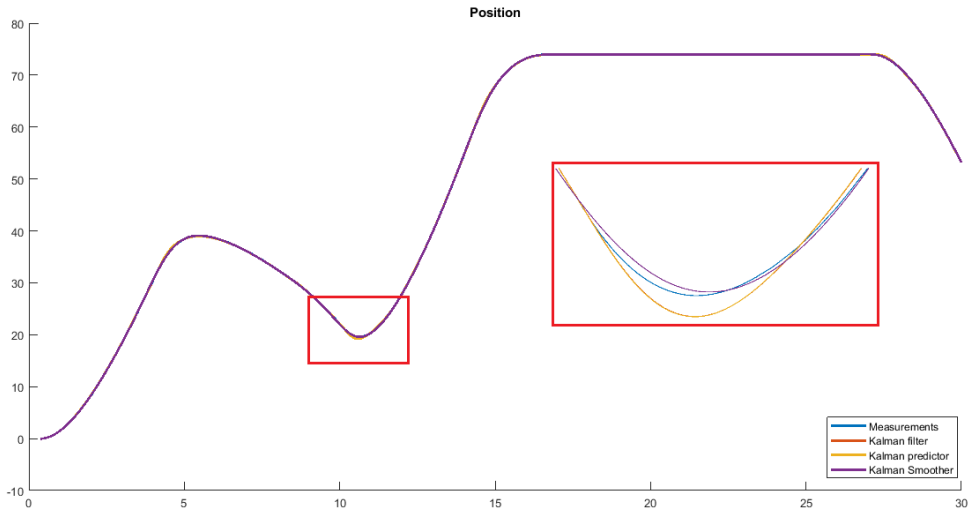

Figure 11: Position comparison between estimation data, Kalman filter, Kalman predictor and Kalman smoother

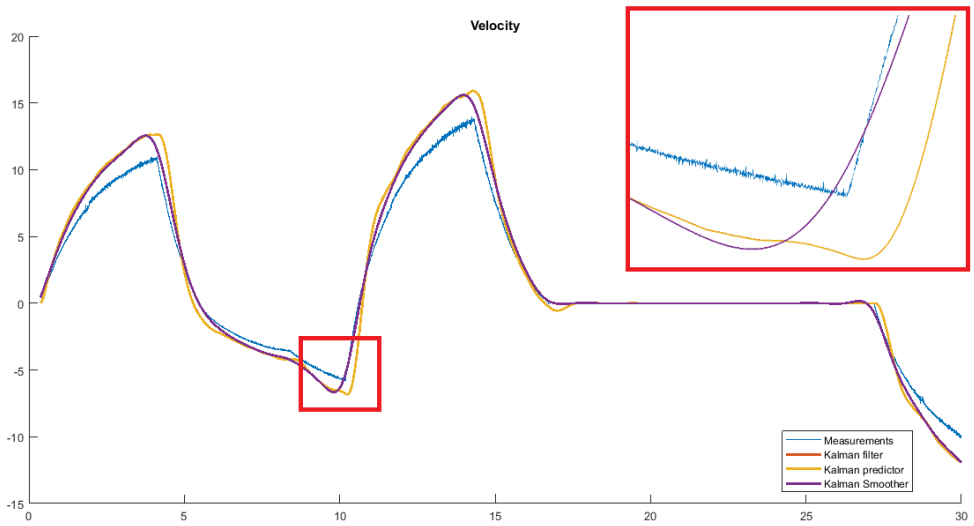

Figure 12: Velocity comparison between estimation data, Kalman filter, Kalman predictor and Kalman smoother

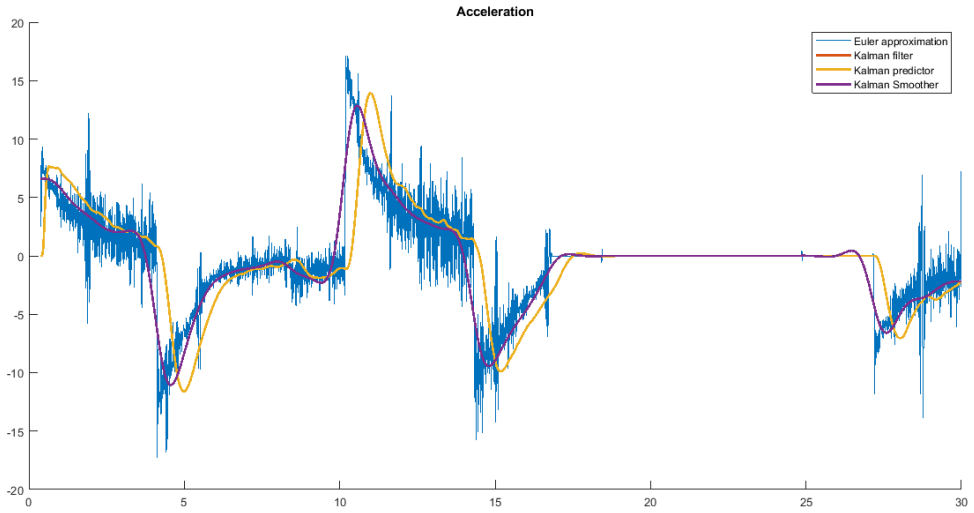

Figure 13: Acceleration comparison between Euler approximation, Kalman filter, Kalman predictor and Kalman smoother

2.2 Steady state Kalman filter and predictor

Description: Implement the steady state Kalman filter/predictor and estimate the velocity and acceleration from noisy position measurements

The following figures compare velocity and acceleration estimated with steady state and not steady state kalman predictor/smoother

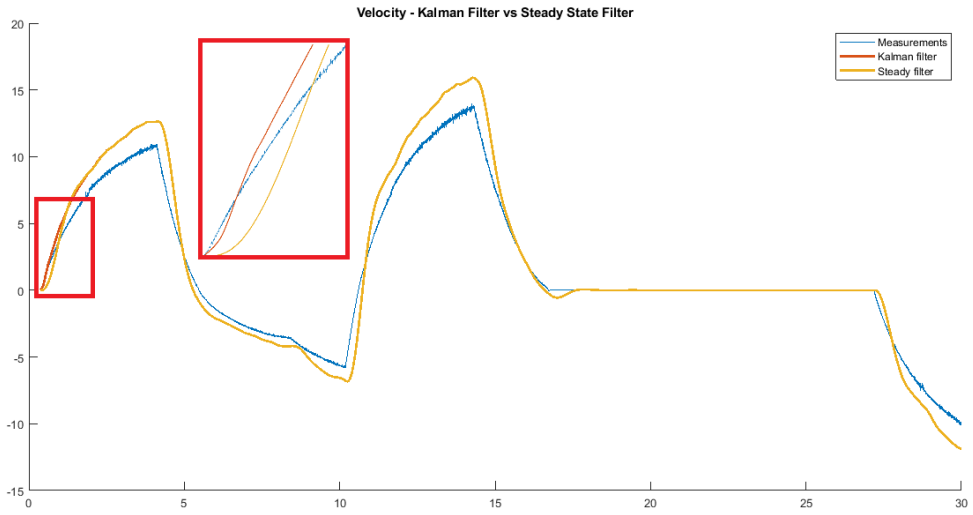

Figure 14: Velocity comparison between estimation data, Kalman filter and steady state Kalman filter

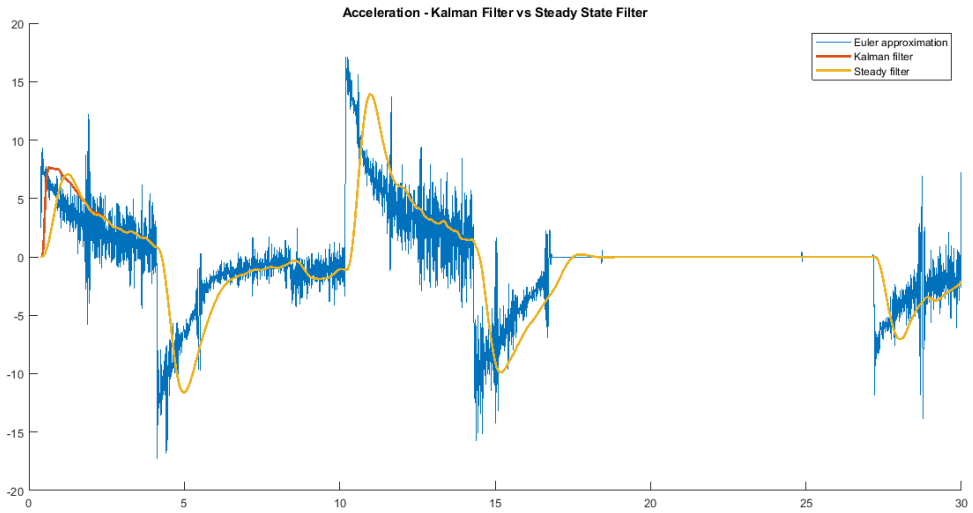

Figure 15: Acceleration comparison between Euler approximation, Kalman filter and steady state Kalman filter

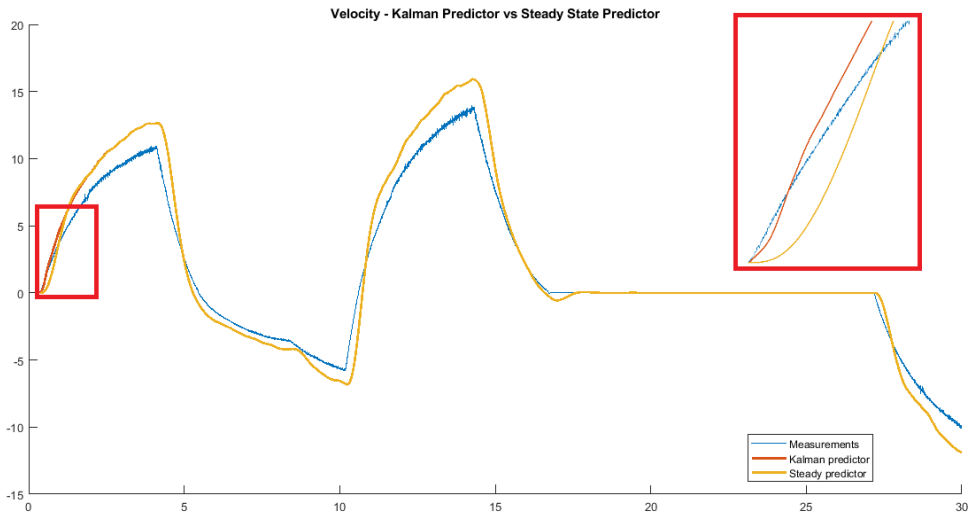

Figure 16: Velocity comparison between estimation data, Kalman predictor and steady state Kalman predictor

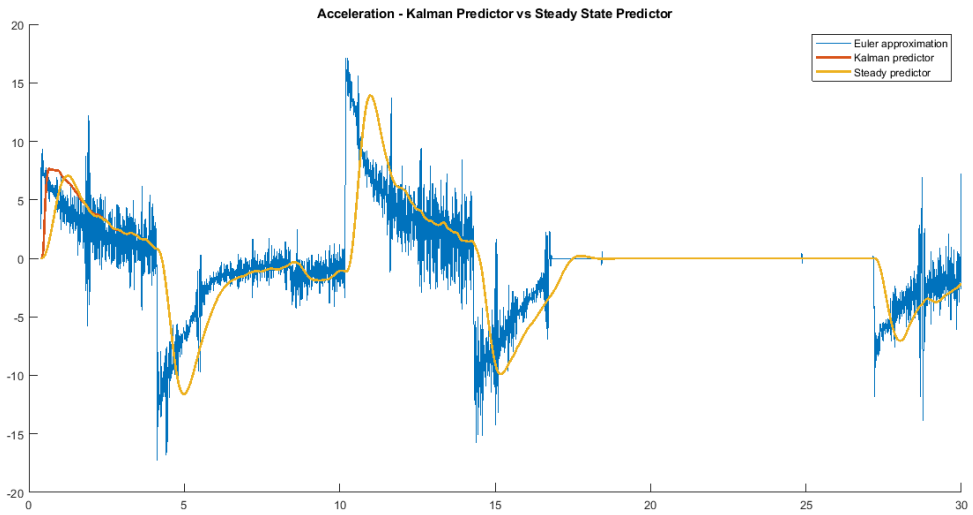

Figure 17: Acceleration comparison between Euler approximation, Kalman predictor and steady state Kalman predictor

3 LS, RLS and Adaptive Estimation

Description: Identify the parameters k and τ using the Least Square, Recursive Least Square on the DC motors data This section reports the result of the following gray-box identification techniques

- Least Squares
- Recursive Least Squares
- Adaptive Algorithm

The model choose was a linear model and in more detail the DC motor model Transfer function

$$P(s) = \frac{\hat{w}(s)}{\hat{V}(s)} = \frac{K_m}{(Js+b)(Ls+R)+K_mK_e} \overset{\text{L=0}}{=} \frac{K_m}{(Js+b)+K_mK_e} = \frac{k}{\tau s+1}$$

Differential equation

$$\tau\dot{w}(t) + w(t) = kV(t)$$

Rewriting the differential equation

$$\frac{\tau}{k}\dot{w}(t) + \frac{1}{k}w(t) = V(t)$$

Let

$$x = [\dot{w},\ w] \quad y = V \quad \theta = [\frac{\tau}{k},\ \frac{1}{k}]'$$

then our linear model can be expressed in the form

$$y = \beta x$$

where β is our vector of unknown we have to estimate

The LS expression for β is given by the following equation

$$\beta = (X^TX)^{-1}X^TY = (\sum_{i=1}^{N} x_i^T x_i)^{-1} \sum_{i=1}^{N} x_i^T y_i$$

where X is the matrix containing the observation data and Y the one containing the predictions

The RLS does not compute β one-shot but recursively calculate β each time a new measurement is recorded

$$RSS_\lambda(\beta(k)) := \sum_{i=1}^{N} \lambda^{k-i}(y_i - x_i\beta_i)^T(y_i - x_i\beta_i)$$

λ is a forgetting factor which allows to estimate time varying-parameters and weight differently the most recent measurements. If it is set to 1 we get no forgetting factors.

The adaptive algorithm minimize the squared error and moves in the opposite direction of the gradient. It computes β at instant k as

$$\beta(k) = \beta(k-1) + gT_s x^T(k)e(k)$$

with T_s the sampling time and $e(k) = y(k) - x(k)$ the error at time k

The following figure show the estimation of the DC motor parameters using LS, RLS, and the adaptive algorithms. The forgetting factor λ of the RLS algorithm was set to 1. The parameter g of the adaptive algorithm was set to 0.3.

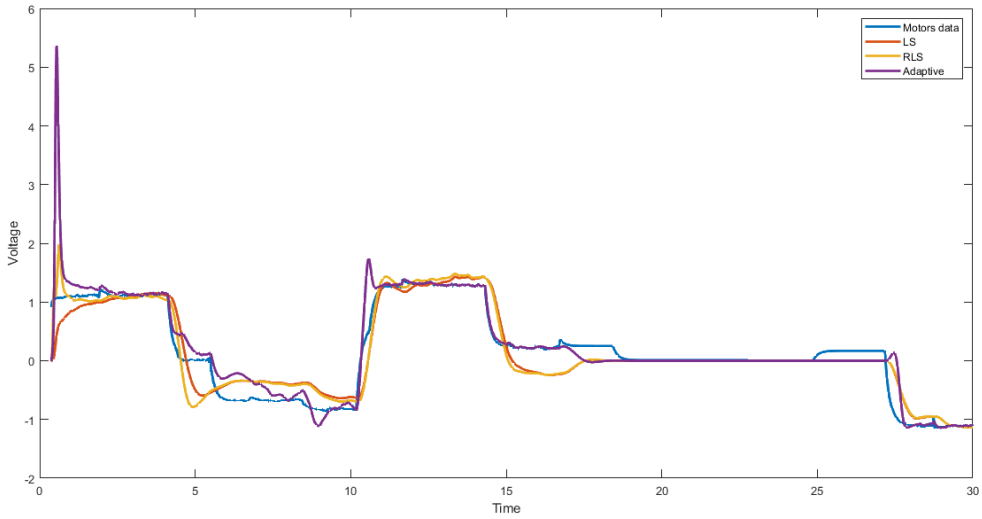

Figure 18: Comparison between LS, RLS and adaptive algorithm, $\lambda = 1$

The estimated parameters were respectively $k = 11.8886$ and $\tau = 0.7138$

The following figure shows the behaviour of the RLS method when λ is set to 0.6;

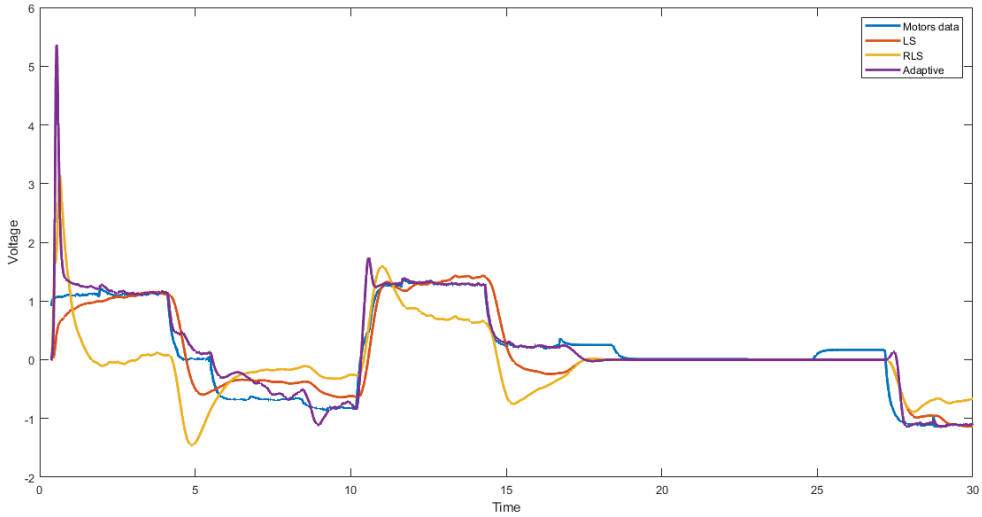

Figure 19: Comparison between LS, RLS and adaptive algorithm, $\lambda = 0.6$

As can be seen, the RLS algorithm is less responsive to adapt to the measurements since at every iteration the last measure is weighted in a lesser manner w.r.t. using $\lambda = 1$

4 Scattering based bilateral teleoperation architecture

Description: Implement the Scattering-based bilateral teleoperation architecture for the

- Force-Position case
- Position-Position case

Compare positions, velocities, forces, commands in free motion and in contact. Add the measurement noise to the position/force signals, and estimate velocities from positions

Architecture parameters

The environment was set at $x = 0.5$, the amplitude of the signals in free motion is 0.3, the amplitude of the signal in contact is 0.8

The architecture was evaluated with a delay of 10 time steps in the communication channel, the environment was modelled as $B_e = 20, K_e = 210$

The wave transformation parameter b was set to 1

A low pass filter with cutoff frequency $8Hz$ was introduced in the communication channel

4.1 Force-Position

Here are reported the wave transformation formulas in the force position case

$$u_m = \sqrt{2b}\dot{x}_m + v_m \quad u_s = \sqrt{\frac{2}{b}F_s} - v_s$$

$$F_m = b\dot{x}_m + \sqrt{2b}v_m \quad \dot{x}_s = -\frac{1}{b}(F_s - \sqrt{2b}v_s)$$

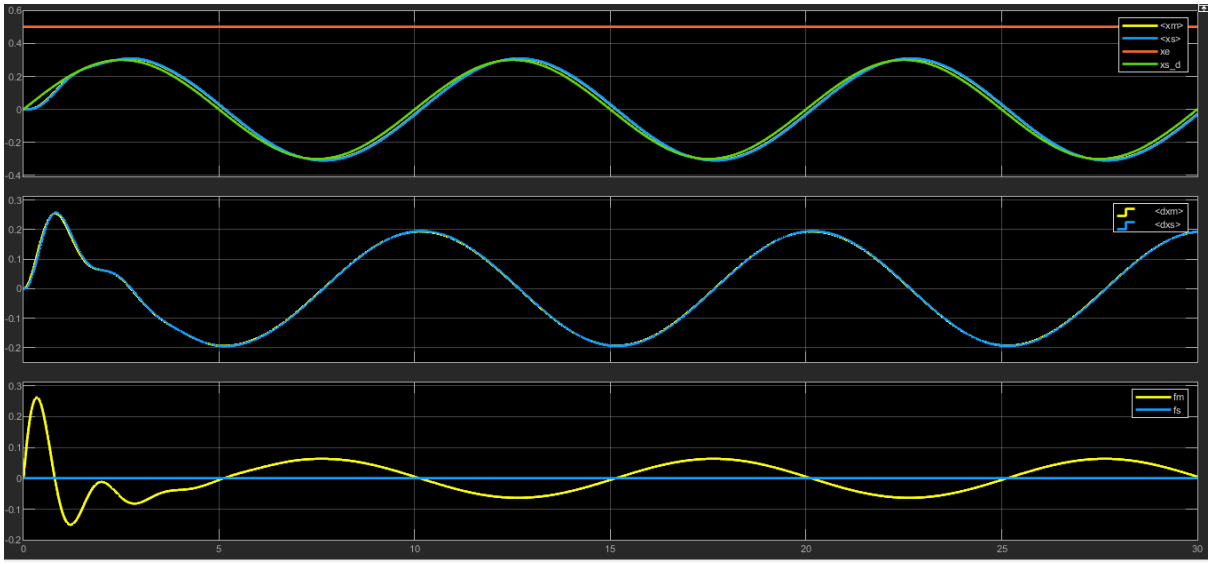

Figure 20: Scattering based bilateral teleop force-position with a sinuisoidal reference signal in free motion, sin frequency $= \pi$

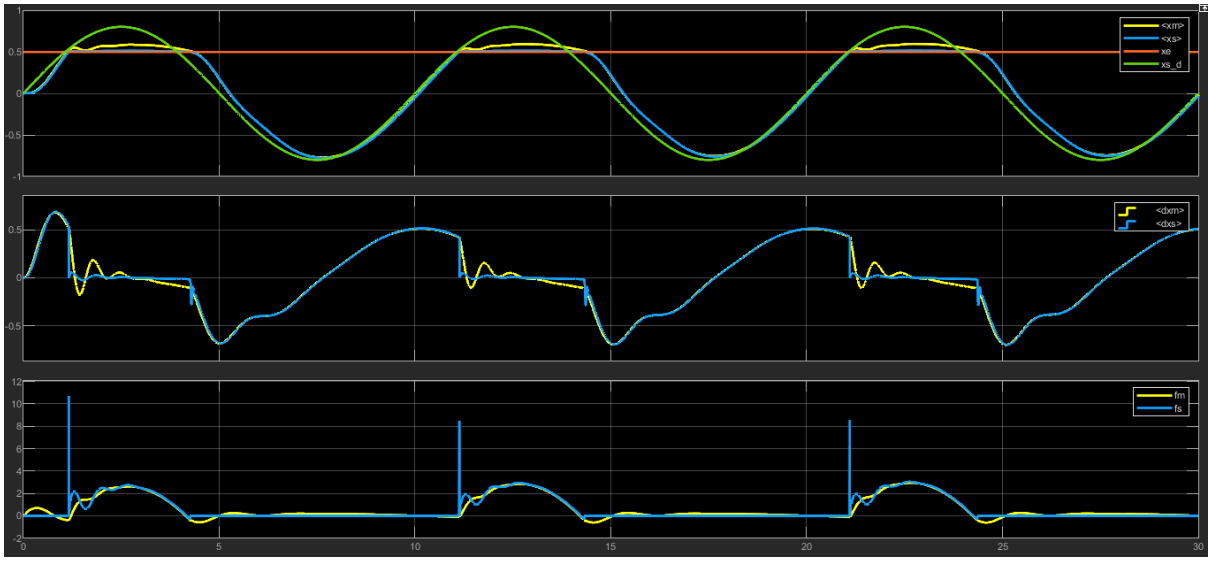

Figure 21: Scattering based bilateral teleop force-position with a sinuisoidal reference signal in contact, sin frequency $= \pi$

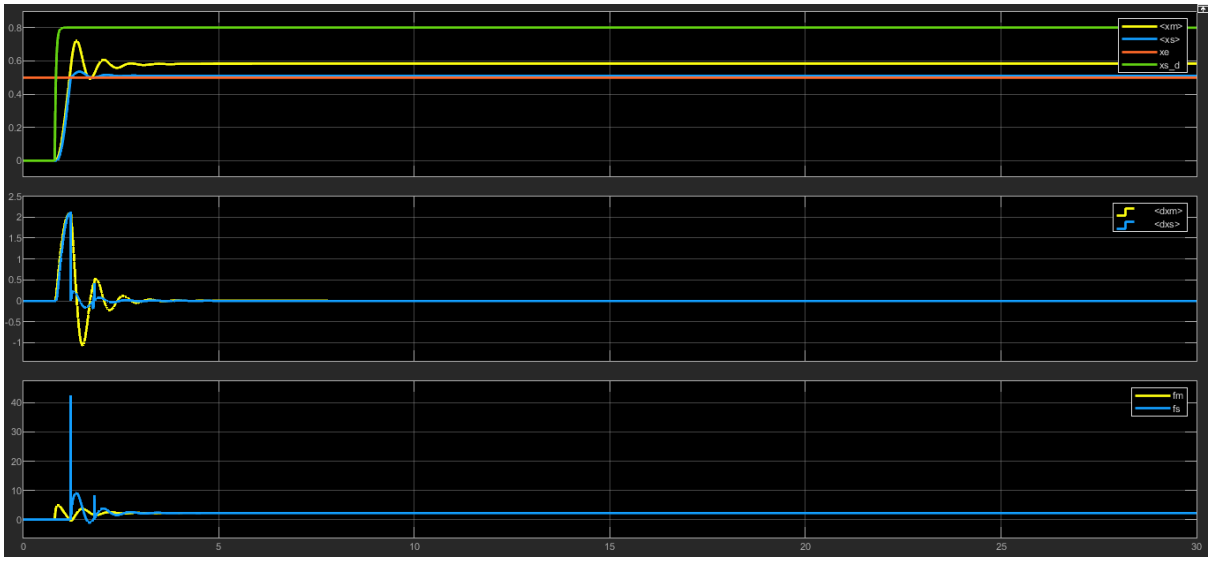

Figure 22: Scattering based bilateral teleop force-position with a step reference signal in contact. To obtain the response, the integral action from the human intention controller was removed

4.2 Force-Position with measurement noise and velocity estimation

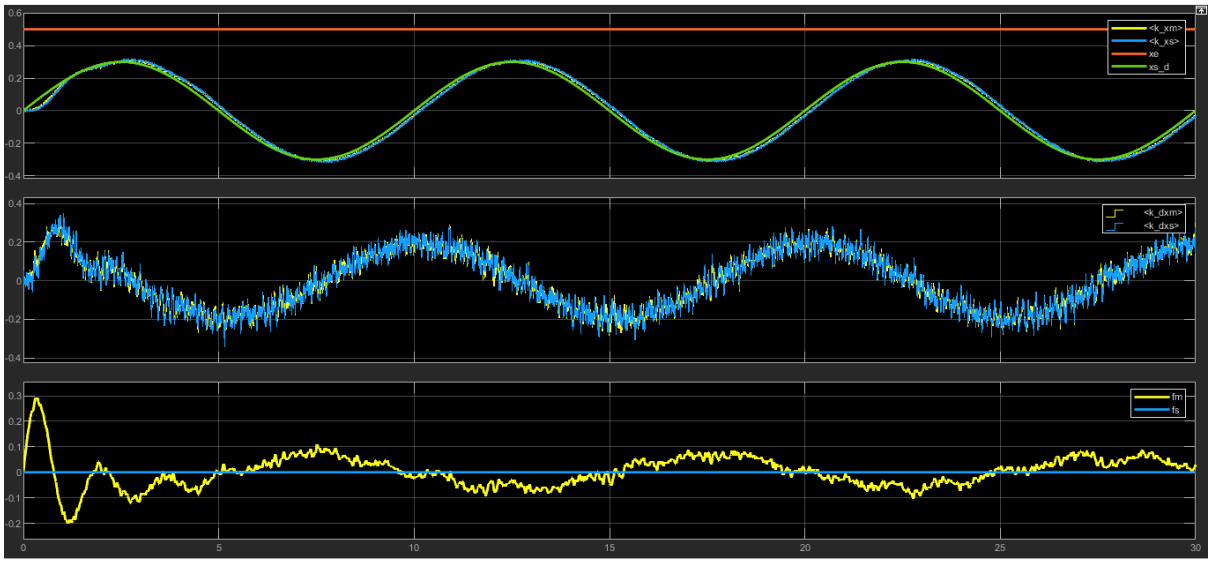

Figure 23: Scattering based bilateral teleop force-position with a sinuisoidal reference signal in free motion, sin frequency $= \pi$

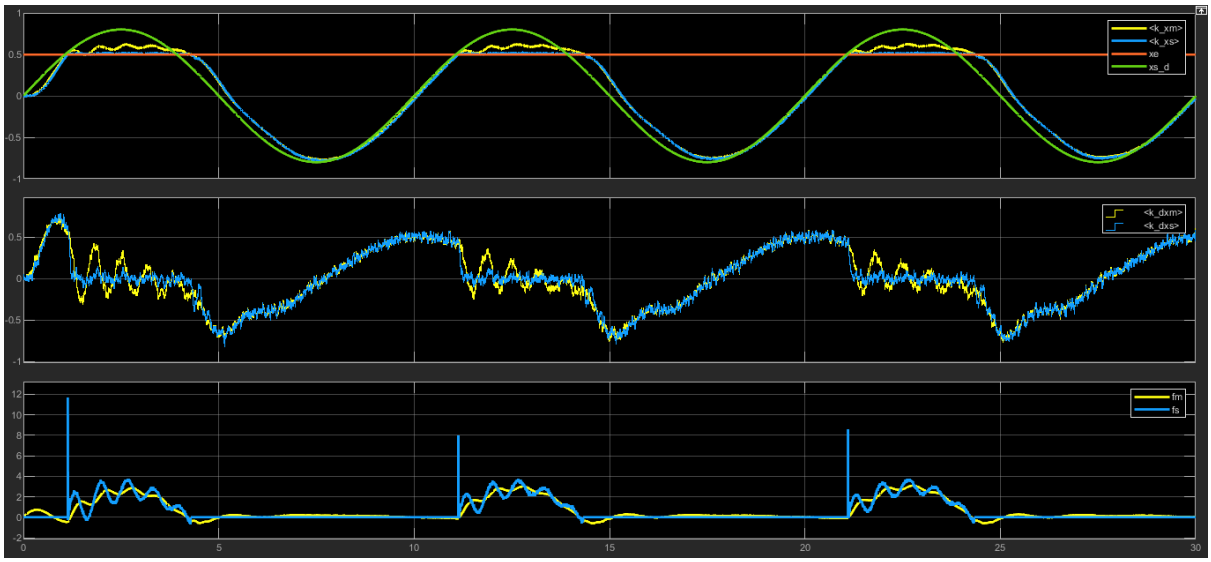

Figure 24: Scattering based bilateral teleop force-position with a sinuisoidal reference signal in contact, sin frequency $= \pi$

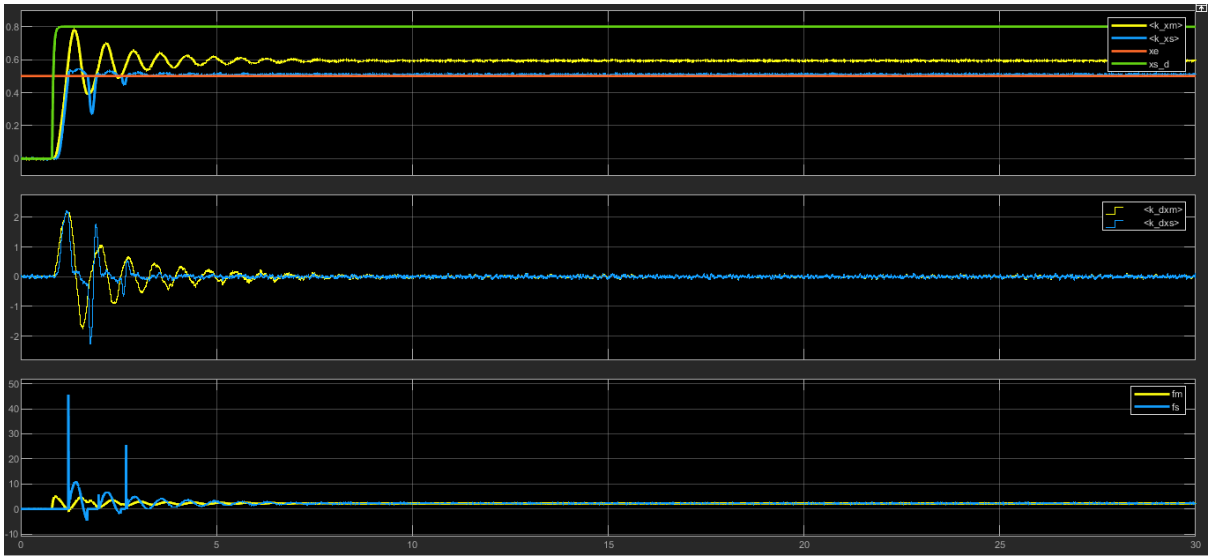

Figure 25: Scattering based bilateral teleop force-position with a step reference signal in contact. To obtain the response, the integral action from the human intention controller was removed

4.3 Position-Position

Here are reported the wave transformation formulas in the force position case

$$u_m = \sqrt{\frac{2}{b}} F_m - v_m \quad u_s = \sqrt{\frac{2}{b}} F_s - v_s$$
$$\dot{x}_m = \frac{1}{b}(F_m - \sqrt{2b} v_m) \quad \dot{x}_s = -\frac{1}{b}(F_s - \sqrt{2b} v_s)$$

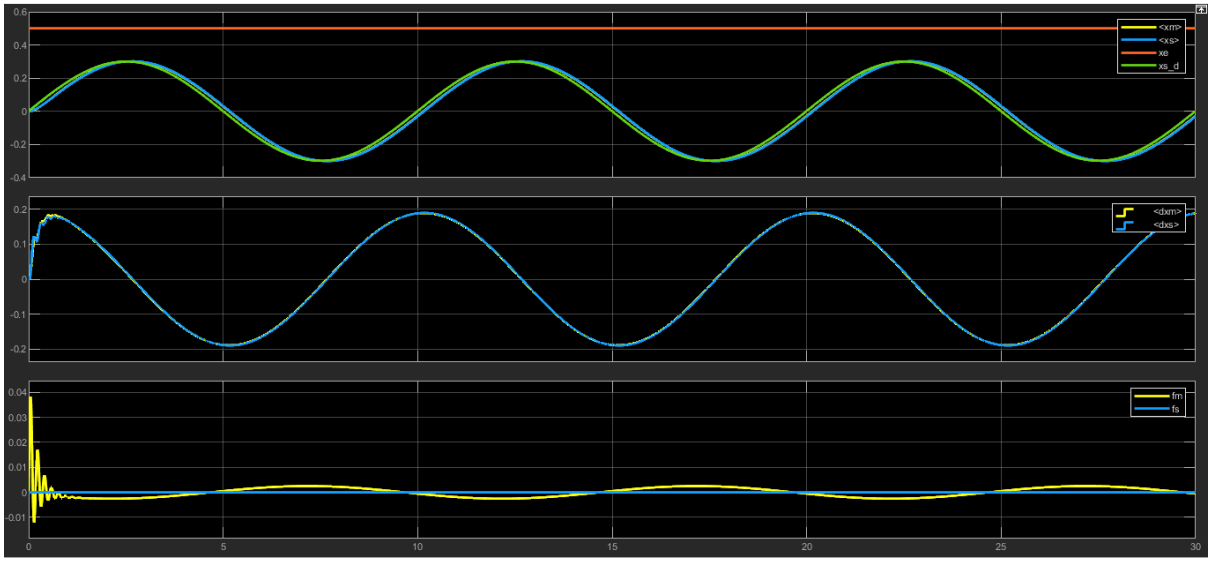

Figure 26: Scattering based bilateral teleop position-position with a sinuisoidal reference signal in free motion, sin frequency $= \pi$

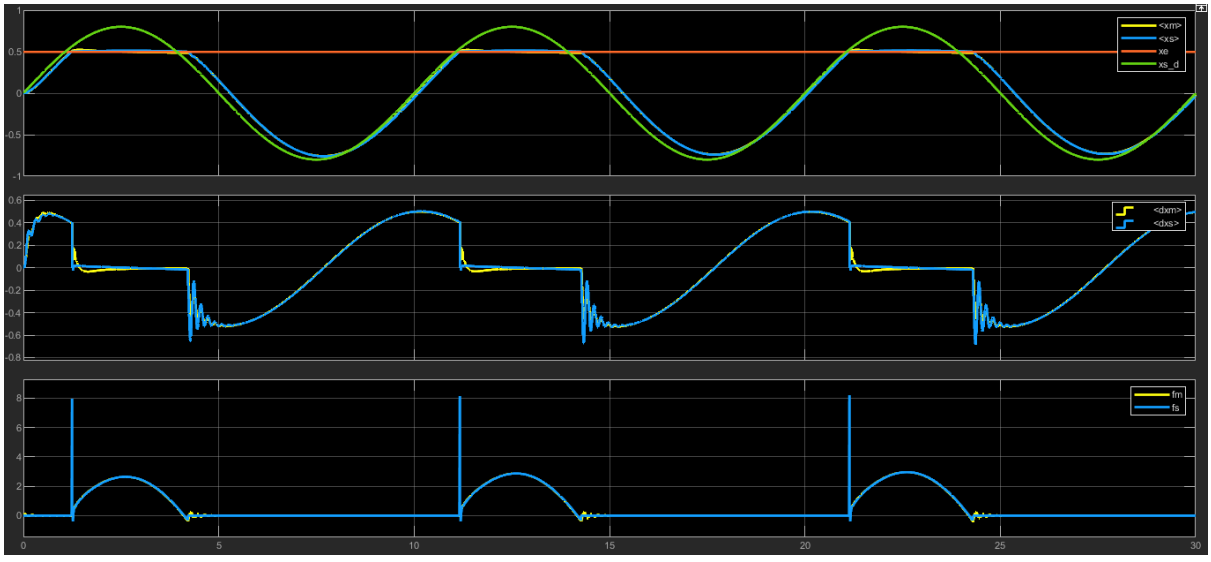

Figure 27: Scattering based bilateral teleop position-position with a sinuisoidal reference signal in contact, sin frequency $= \pi$

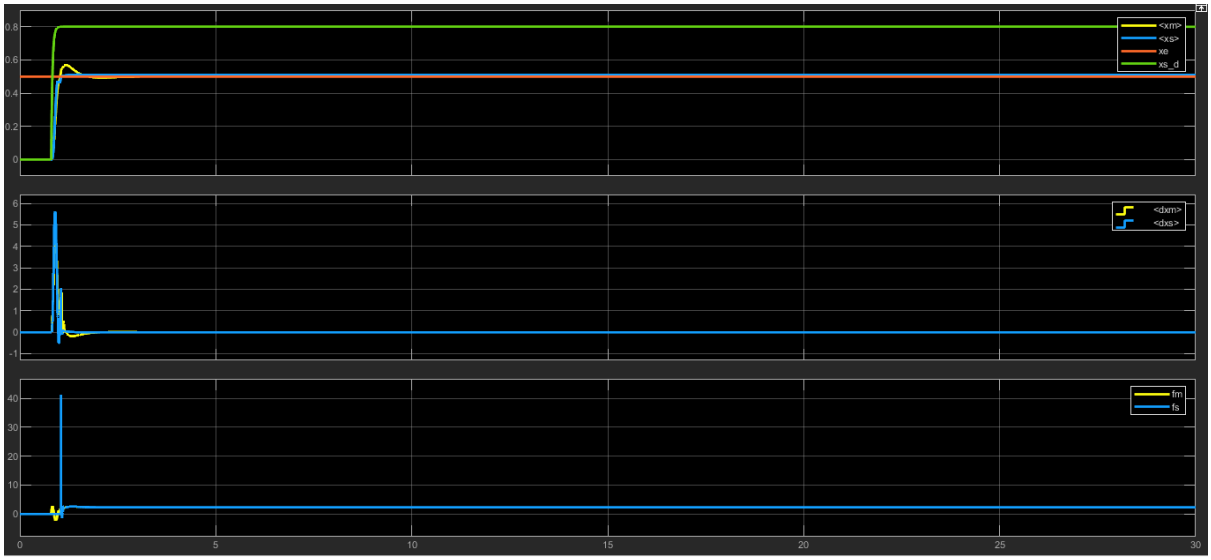

Figure 28: Scattering based bilateral teleop position-position with a step reference signal in contact. To obtain the response, the integral action from the human intention controller was removed

4.4 Position-Position with measurement noise and velocity estimation

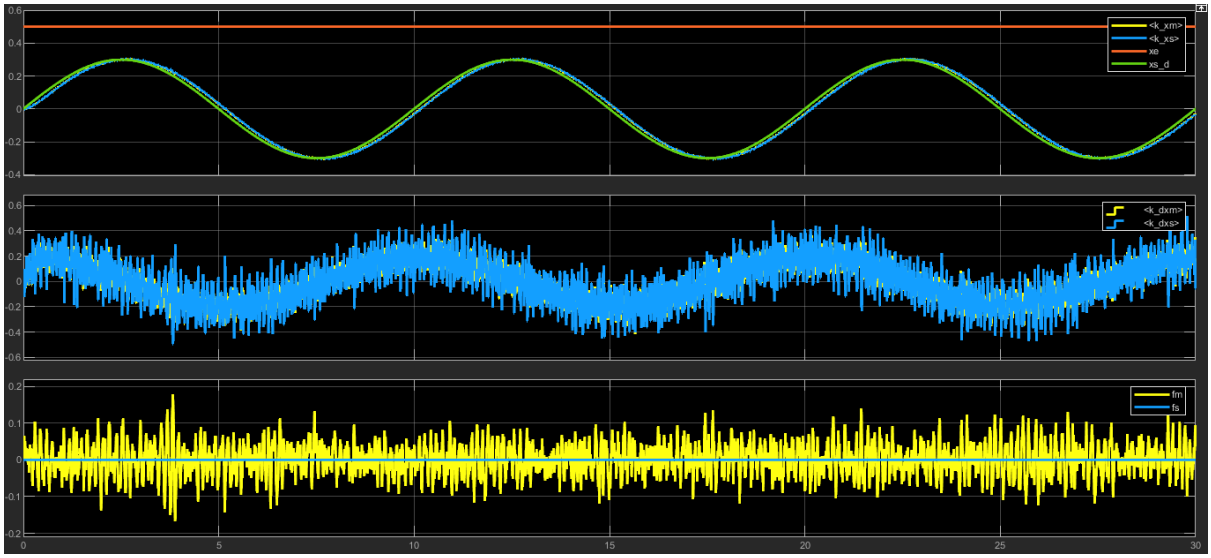

Figure 29: Scattering based bilateral teleop position-position with a sinuisoidal reference signal in free motion, sin frequency $= \pi$

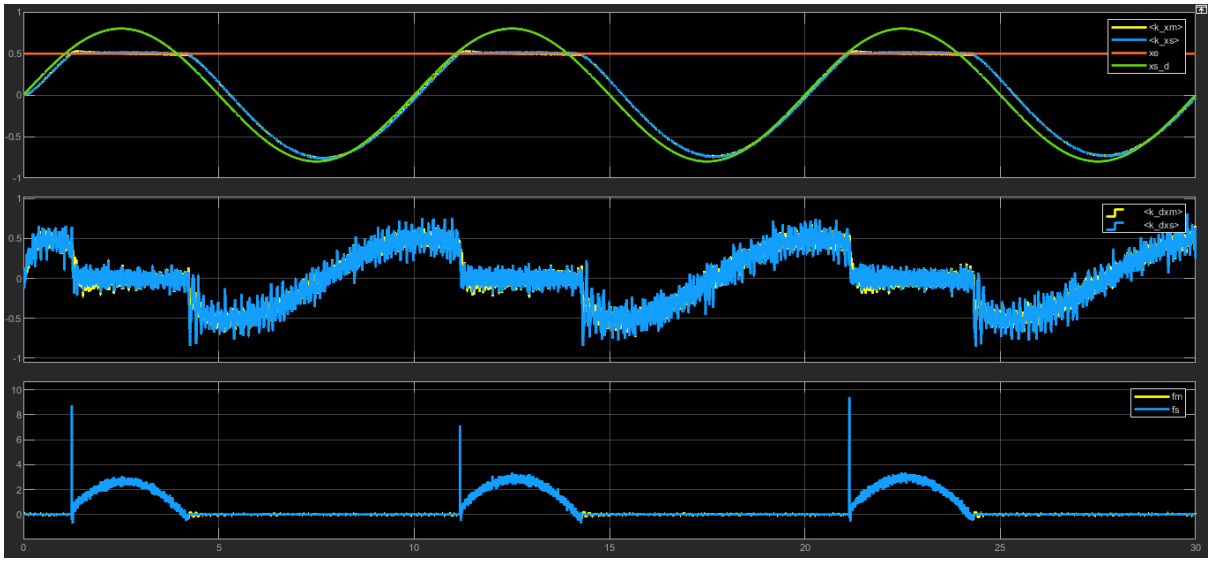

Figure 30: Scattering based bilateral teleop position-position with a sinuisoidal reference signal in contact, sin frequency $= \pi$

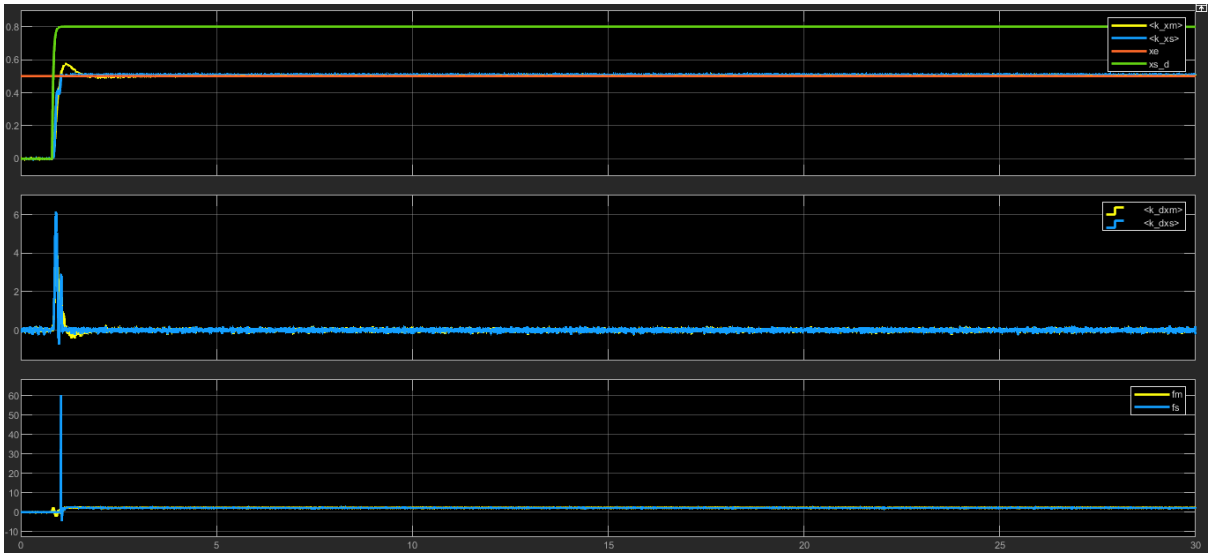

Figure 31: Scattering based bilateral teleop position-position with a step reference signal in contact. To obtain the response, the integral action from the human intention controller was removed

5 Tank based bilateral teleoperation architecture

The tank based bilateral teleoperation architecture implements a two-layer approach: The hierarchical top layer is used to implement a strategy that addresses the desired transparency, and the lower layer ensures that no "virtual"energy is generated. The architecture does not need any about the time delay in the communication channel which can be also time-varying. The main concept of this architecture is the presence of two communication energy storage tanks from which the motions of both the slave and the master are powered.

Transparency layer: control structure which is implemented to provide the best possible transparency of the telemanipulation chain, taking into account all available information about the system, the environment, and the task the user is executing

Passivity layer: given the command computed by the transparency layer, this layer contains an algorithm to maintain passivity of the total system.

The level of these tanks can be interpreted as a tight energy budget from which controlled movements can be powered and which are being replenished by the user at the master side when necessary or if possible/desired also at the slave side

At each discrete instant, the energy at each side is computed by the following equations

$$H(k) = H(\overline{k}) + H_{+}(k) - \Delta H_I(k)$$

where $H(\overline{k})$ is the energy from at the previous time instant, $H_{+}(k)$ is the sum of the energy received from the other side, and $H_I(k)$ is the energy used at time k computed in the following manner

$$\Delta H_I(k) = \tau(\overline{k})\Delta q(k)$$

The energy level for the next time instant is computed by

$$H(\overline{k+1}) = H(k) - H_{-}(k)$$

$H_{-}(k)$ is the energy exchanged at each time instant computed as $H_{-}(k) = \beta H(k)$ with $\beta < 0$. The computation of the saturated controlled torque is omitted

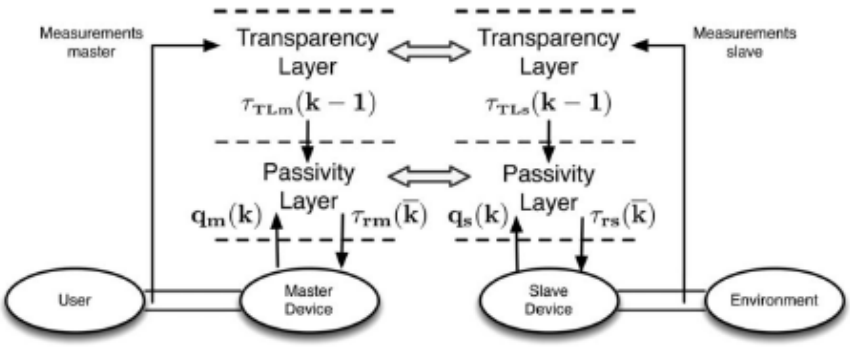

Figure 32: Tank based bilateral teleop architecture

Description: Implement the Tank-based bilateral teleoperation architecture for the

- Force-Position case
- Position-Position case

Compare positions, velocities, forces, commands in free motion and in contact. Add the measurement noise to the position/force signals, and estimate velocities from positions

Architecture parameters

The environment was set at $x = 0.5$, the amplitude of the signals in free motion is 0.3, the amplitude of the signal in contact is 0.8

The architecture was evaluated with a delay of 10 time steps in the communication channel, the environment was modelled as $B_e = 20, K_e = 210$

Enough initial energy was provided to the tanks at the slave and master side to allow the motion of the two systems

5.1 Force-Position

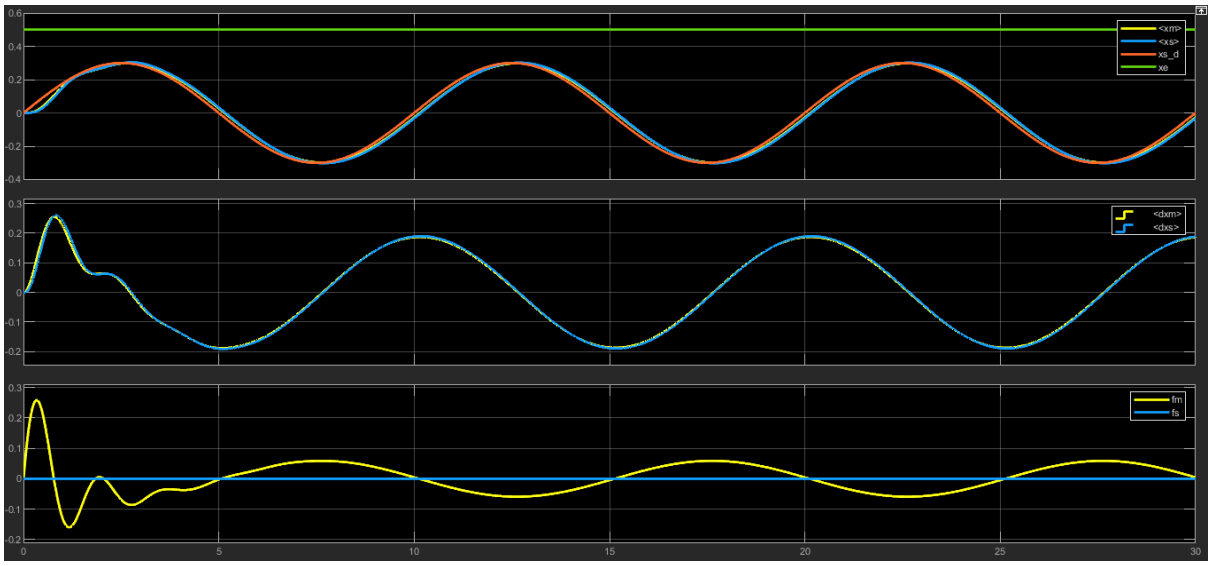

Figure 33: Tank based bilateral teleop force-position with a sinuisoidal reference signal in free motion, sin frequency $= \pi$

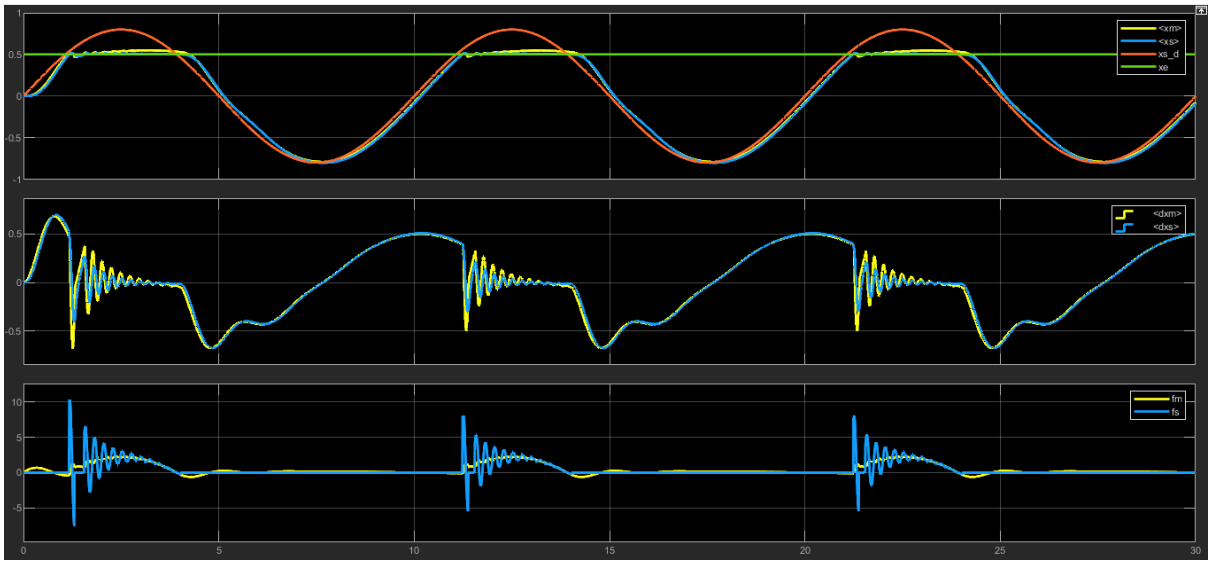

Figure 34: Tank based bilateral teleop force-position with a sinuisoidal reference signal in contact, sin frequency $= \pi$

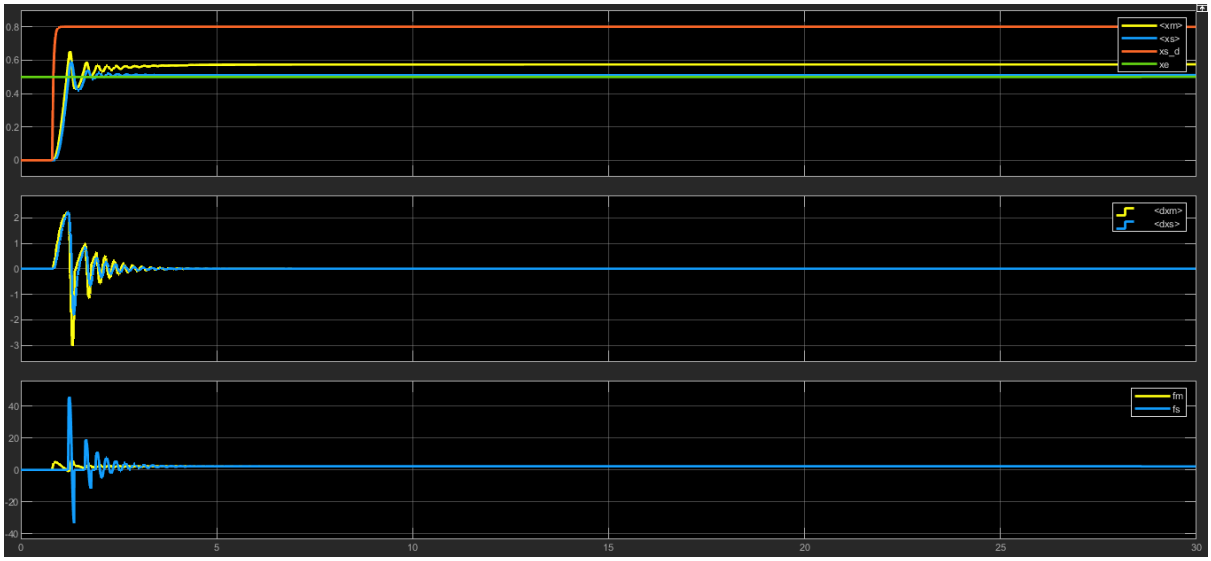

Figure 35: Tank based bilateral teleop force-position with a step reference signal in contact

5.2 Force-Position with measurement noise and velocity estimation

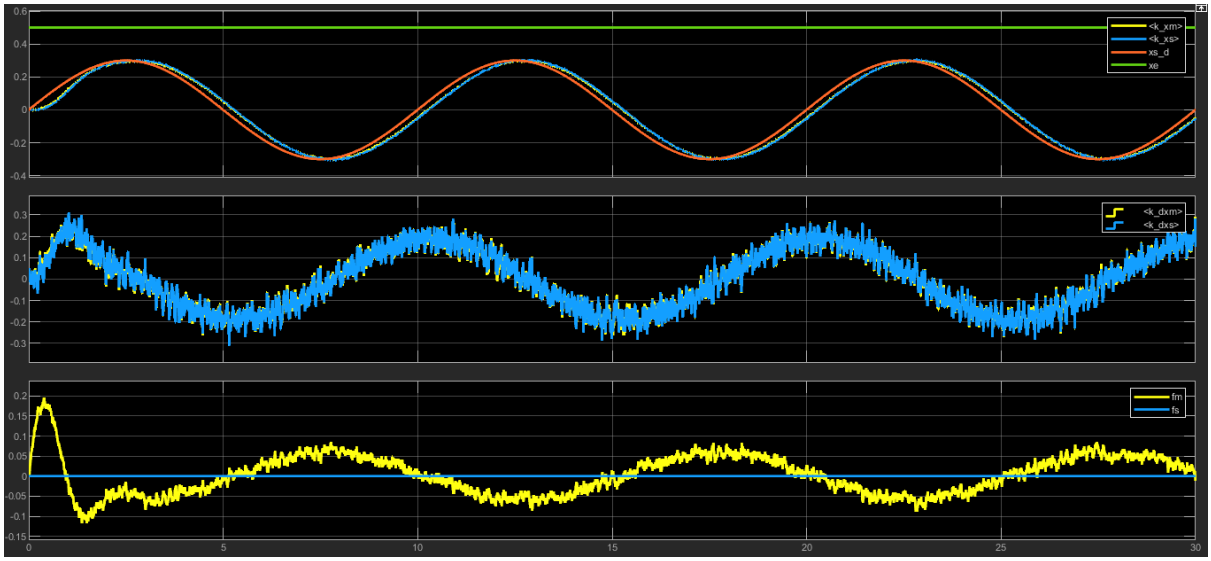

Figure 36: Tank based bilateral teleop force-position with a sinuisoidal reference signal in free motion, sin frequency $= \pi$

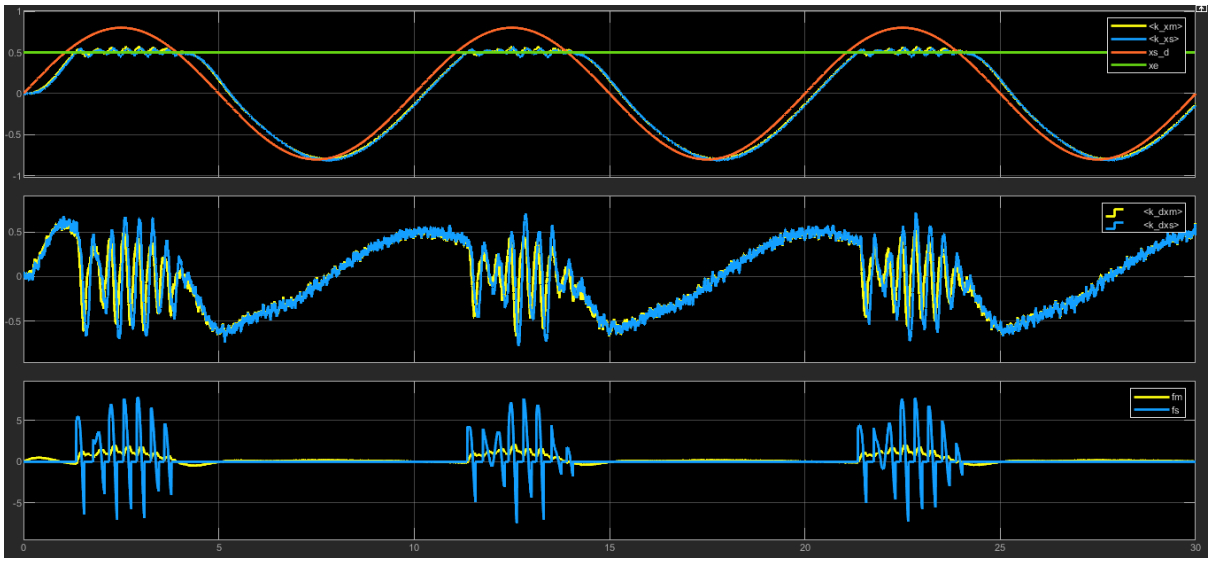

Figure 37: Tank based bilateral teleop force-position with a sinuisoidal reference signal in contact, sin frequency $= \pi$

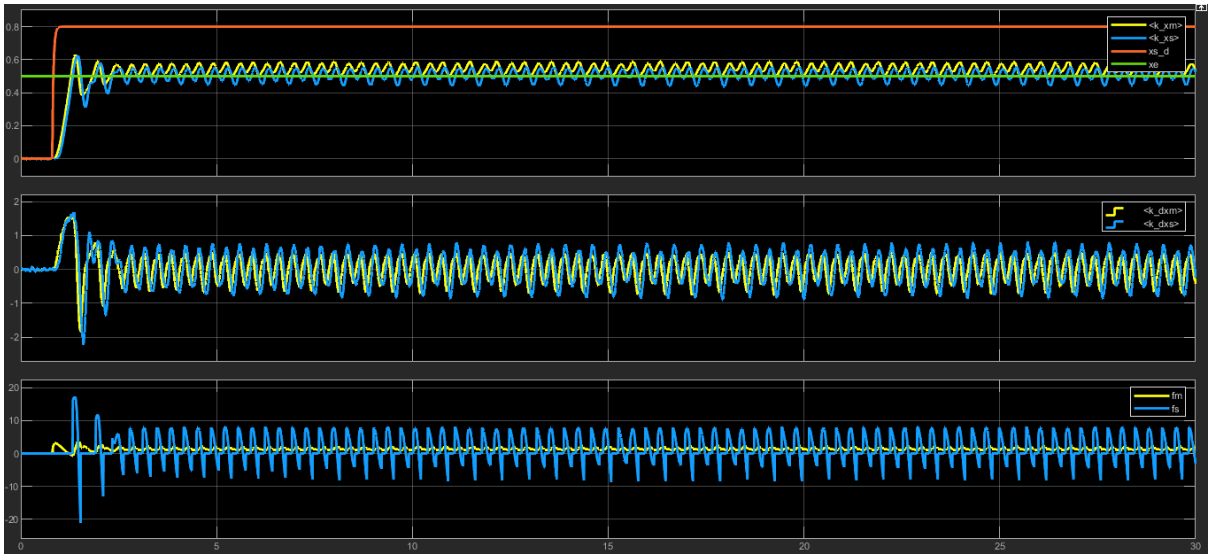

Figure 38: Tank based bilateral teleop force-position with a step reference signal in contact

5.3 Position-Position

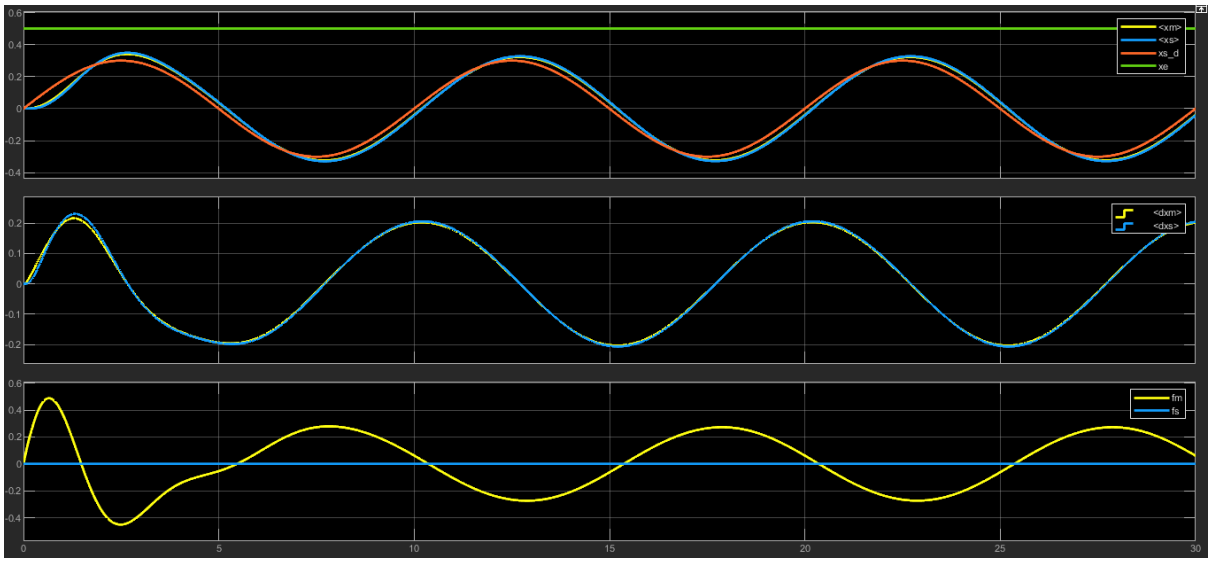

Figure 39: Tank based bilateral teleop position-position with a sinuisoidal reference signal in free motion, sin frequency $= \pi$

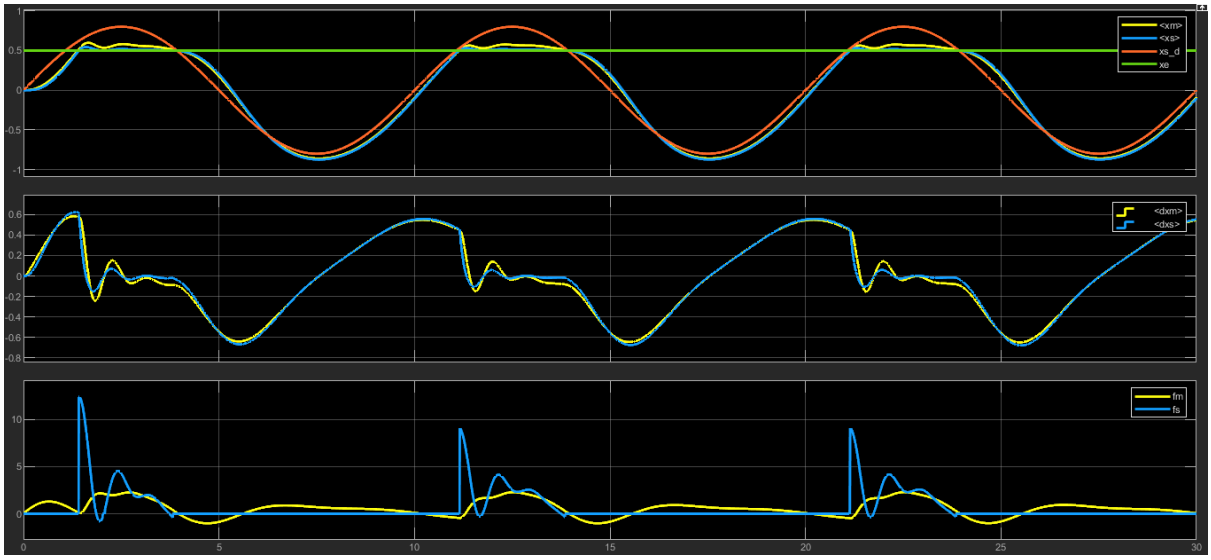

Figure 40: Tank based bilateral teleop position-position with a sinuisoidal reference signal in contact, sin frequency $= \pi$

Figure 41: Tank based bilateral teleop position-position with a step reference signal in contact

5.4 Position-Position with measurement noise and velocity estimation

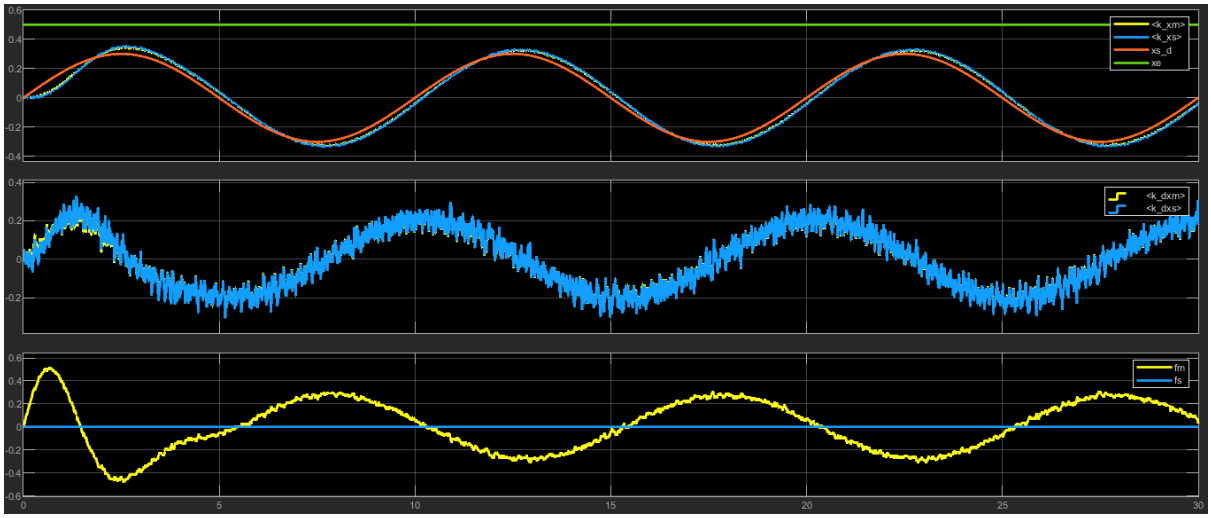

Figure 42: Tank based bilateral teleop position-position with a sinuisoidal reference signal in free motion, sin frequency $= \pi$

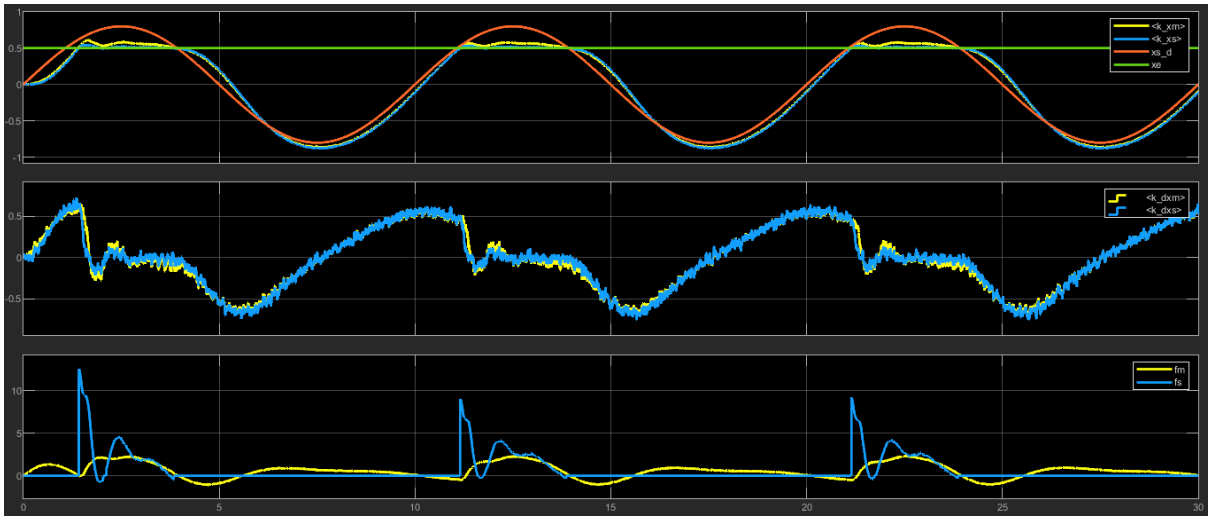

Figure 43: Tank based bilateral teleop position-position with a sinuisoidal reference signal in contact, sin frequency $= \pi$

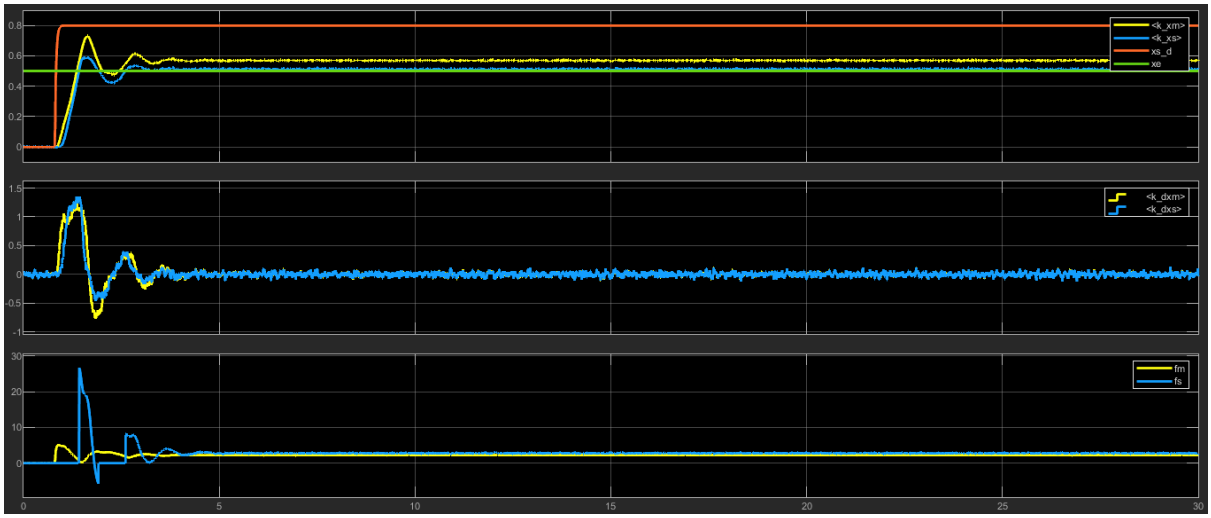

Figure 44: Tank based bilateral teleop position-position with a step reference signal in contact